

A Comparative Study of Groundwater Recharge Mapping Using Analytical Hierarchy Process, Fuzzy-Analytical Hierarchy Process, and Frequency Ratio Models: A Case Study from Quetta Region, Pakistan

Ali, I.,^{1,2*} Khatibi, B. M.¹ and Karimzadeh, S.¹

¹Department of Remote Sensing and GIS, University of Tabriz, Tabriz, Iran

²Department of Geological Engineering, Balochistan University of Information Technology, Engineering and Management Sciences (BUIITEMS), Quetta, Pakistan, E-mail: imadali_khan@yahoo.com*

*Corresponding Author

DOI: <https://doi.org/10.52939/ijg.v20i7.3411>

Abstract

Groundwater is an essential resource in arid and semi-arid regions, where water scarcity and droughts are common. The Quetta region of Pakistan is one such area that requires effective groundwater recharge zone mapping to manage groundwater resources adequately. This study aimed to delineate groundwater recharge zones using analytical hierarchy process (AHP), fuzzy-AHP, and frequency ratio (FR) models. Additionally, it aimed to compare the effectiveness of these models in groundwater recharge potential zone mapping. To achieve the objectives, nine groundwater influencing factors were considered: geology, soil types, lineament density, elevation, slope, topographic wetness index, drainage density, land use land cover, and rainfall. Thematic maps for all these factors were generated using satellite and conventional data in the ArcGIS environment. All thematic layers were combined using AHP model-I (Weighed overlay), AHP model-II (Weighted sum), fuzzy-AHP overlay, and FR-based model using ArcGIS. The findings revealed that 15% and 39% of the study area have high recharge potentials according to AHP-based model-I and model-II, respectively. The FAHP model demarcated 43% of the area as high recharge zones, while the FR model demarcated 42% as high recharge zones. The majority of high groundwater recharge areas were found in the central part of the study area, while the southern part was demarcated as a moderate recharge zone. The eastern and western parts were demarcated as low recharge potential zones. To validate the accuracy of the models, the study used receiver operating characteristic (ROC) validation curves. The ROC curves revealed that AHP model-II had the highest accuracy (AUC=89%), followed by the FAHP model (AUC=88%), AHP model-I (AUC=84%), and FR (AUC=81%). In conclusion, the AHP model-II was more effective in recharge zone demarcation than the FAHP and FR models in the current study. The results of this study can benefit decision-makers in groundwater resource management and future planning in land use for urban extension, particularly in water-scarce regions of the country.

Keywords: Analytical Hierarchy Process, Frequency Ratio, Fuzzy-Analytical Hierarchy Process, Groundwater Recharges Zoning, Quetta Region

1. Introduction

Water is a very critical source of life indeed. Certainly, population evolution, aging infrastructure, climate change, and an upsurge in strict water quality standards are the main aspects that evidence it [1] and [2]. Despite its importance, water is a poorly managed natural resource on the earth's planet [3]. Groundwater (GW) is a type of water present in subsurface fractured lithological formations and soil pores [4]. In both developed and developing countries worldwide, GW has emerged as a vital and reliable source of water for both urban and rural areas [5]. GW is the foremost source of

water for irrigation and agricultural activities worldwide. It is worth noting that more than 60% of agricultural practices are dependent on GW [6]. Pakistan ranks fourth in the world in terms of the amount of GW extracted for irrigation purposes. Only 27% of the entire agriculture area is irrigated by surface water supplies, while the remaining 73% depends on GW either directly or indirectly. Presently, around 1.2 million private tube wells abstracting GW in the country, having an annual abstraction rate of around 65 billion cubic meters [7].

Baluchistan province is situated in an arid to semi-arid climatic zone of Pakistan. In this area, the source of surface water is non-perennial, which means that GW is the only dependable source for municipal, industrial, and agricultural usage [8][9] and [10]. Agriculture is the key pillar of the economy of about 85% population of the province [11]. The province was hit by numerous severe droughts in history, which had a radical influence on livelihoods and its economy and destroyed around 80% of its fruit orchards [12]. Over 40% of the population of the province resides in the Pishin basin, with most living in and around the Quetta region (study area). Over the course of the last decade, the population of the Quetta region has experienced a significant increase from 1.02 million to 1.8 million individuals. The escalation of population density has been observed to correlate with a subsequent surge in the demand for agricultural and industrial water, ultimately leading to an exacerbation of water scarcity in the study area. This phenomenon highlights a significant challenge that needs to be addressed, as it poses a serious threat to the sustainable management of water resources [13].

Research reveals that if the watersheds are not managed in an integrated sustainable way, led to a diminution of natural resources i.e., water, vegetation, soil fertility, flora and fauna, etc. [14]. Understanding the scenario of GW resources is crucial for ensuring sustainable development in a region [1]. The GW recharge potential mapping and delineation is among the most important and prior stages in GW resources management and planning [15]. The utilization of geospatial technologies is essential for the successful exploration of groundwater and the effective management of watersheds. These innovative technologies enable the measurement, analysis, and visualization of geospatial data, thus facilitating the identification of water resources and the monitoring of hydrological processes. As such, geospatial technologies play a crucial role in the evaluation and management of water resources, aiding decision-makers in making informed and effective decisions that ensure sustainable water use. Geospatial technologies are more efficient and cost-effective alternative to traditional methods. They allow for quicker completion of tasks, while also reducing overall costs [4][16] and [17]. GIS coupled with multi criteria decision analysis(MCDA) covers a large area in a short period to map and identify GW recharge potential zones [18]. Several researchers around the globe [18][19][20][21][22][23][24][25][26][27][28][29][30] and [31] have applied GIS and

RS based techniques for identification of GW recharge potential zones. They used GIS-based models like the Analytical hierarchy process (AHP), Fuzzy logic, Frequency ratio (FR), Multi-criteria decision analysis, Shannon's Entropy (SE), etc.

A truly little geospatial technology-based approach has been adopted at country level as well as in the study area. This study employs geospatial technology for delineation of GW recharge potential zones in the Quetta region of Pakistan. In current study we will utilize remote sensing (RS) and geographic information system (GIS) along with the analytical hierarchy process (AHP), fuzzy-AHP, and frequency ratio (FR) models for GW recharge mapping in a drought-prone region. Mapping GW recharge potential zones will assist decision-makers in GW resource management and future land use planning. In drought-prone regions where the GW table is relatively deep, ensuring a consistent supply of clean water has been a significant challenge. This study will also help in the installation of future dug/tube wells or boreholes in the study area which can minimize the cost and effort of hydrogeological investigation.

2. Materials and Methods

2.1 Study Area Description

Baluchistan is the largest province of Pakistan that spreads over an area of about 347,000 km². Geographically, it constitutes about 43% of the total area of the country. Hydrologically, Baluchistan is divided into 18 river basins, namely, Dasht, Gaj, Gawadar, Hab, Hamun-e-Lora, Hingol, Hmun-e-Mashkhel, Kachiplain, Kadnai, Kaha, Kand, Kundar, Mula, Nari, Pishin, Porali, Rakhshan, and Zhob. The Study area of Quetta region is a part of the Pishin River Basin, extends between Latitude from 29°45'00" to 30°30'00", Longitude from 66°45'00 to 67°20'00 (shown in Figure 1).

The topography of the study area is varied and includes elongated mountain ridges, depressions, and small plains. The height of the sub-basin gradually rises as you move towards the northeast of Quetta Valley. This is where the Zarghoon Range is located, forming the highest peak in the area at 3,519 meters above mean sea level (amsl). In Zargoon, the streams flow through gorges with extremely steep slopes. The Takatu Range of 3,401 amsl is exposed in the north, the Chiltan Range is 3,261 amsl exposed in the west and the Murder Ghar is 3,134 amsl exposed to the east of the study area. The central part is somehow flat and gently sloping toward the south along the drainage pattern. The average topographic elevation of the study area is 1,650 amsl.

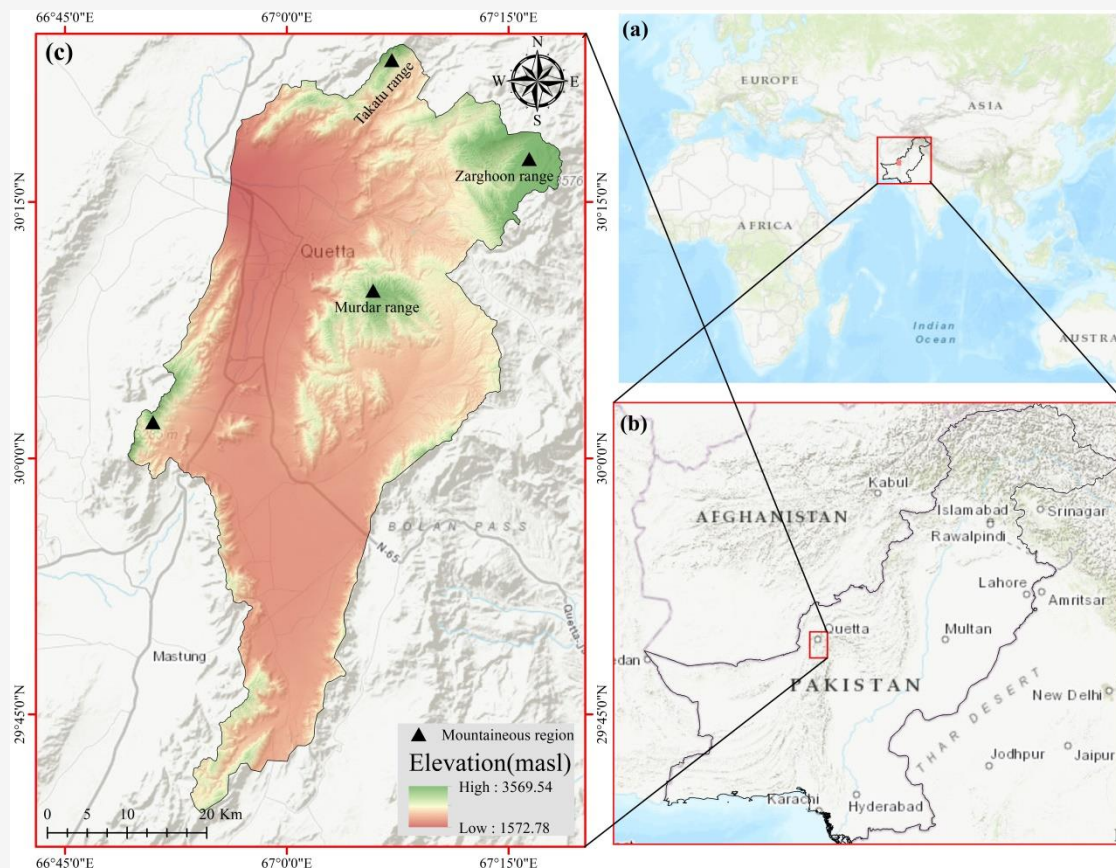


Figure 1: Location map of (a) World (b) Pakistan and (c) Quetta Region

2.2 Data Acquisition Sources and Preparation of Thematic Maps

The acquisition of data is the most critical step in research. The selection of influencing factors is a key stage in GW recharge studies [32] and [33]. In the current study influencing factors were considered based on its importance to the GW recharge and extensive literature review. Thematic maps were constructed from satellite and conventional data by using ArcMap 10.8. A Digital Elevation Model (DEM) with a 30m resolution was downloaded from the open topography website (<https://portal.opentopography.org/>) and was further employed to generate thematic maps, such as slope, elevation, TWI, drainage density. Detail of each thematic layer is discussed in following sections.

2.2.1 Geology

Geology signifies the physical makeup of rocks including their mineral compositions, grain size arrangement, etc. [34]. The type of rock has a significant impact on how groundwater moves because it determines the flow mechanisms and infiltration [35] and [36]. In the current study geological map (1:250000 scale) was collected from

a geological survey of Pakistan, and was rectified and digitized by using ArcGIS-10.8. Ultimately, the thematic map was transformed from vector to raster format prior to assigning weights and ranks (Figure 2(a)).

2.2.2 Lineament Density (LD)

Lineaments provided valuable details on the underground geology and physical characteristics like fractures, faults, and joints. Lineaments express local and regional tectonic behavior; and also act as reservoirs and channels for hydrocarbons and mineral deposits [37]. The lineament map of the study area was generated using the Landsat-8 (Thematic Mapper and Operational Land Imager) satellite image processed with PCI Geomatica Software in PCI Geomatica, the image was imported and improved using the "Enhancements" tool. Subsequently, the Lineament Extraction algorithm from the Algorithm Librarian under Tools was applied. The resulting map was then imported into ArcGIS, and the lineament density was calculated using the Spatial Analyst Tools > Density > Line Density option (Figure 2(b)).

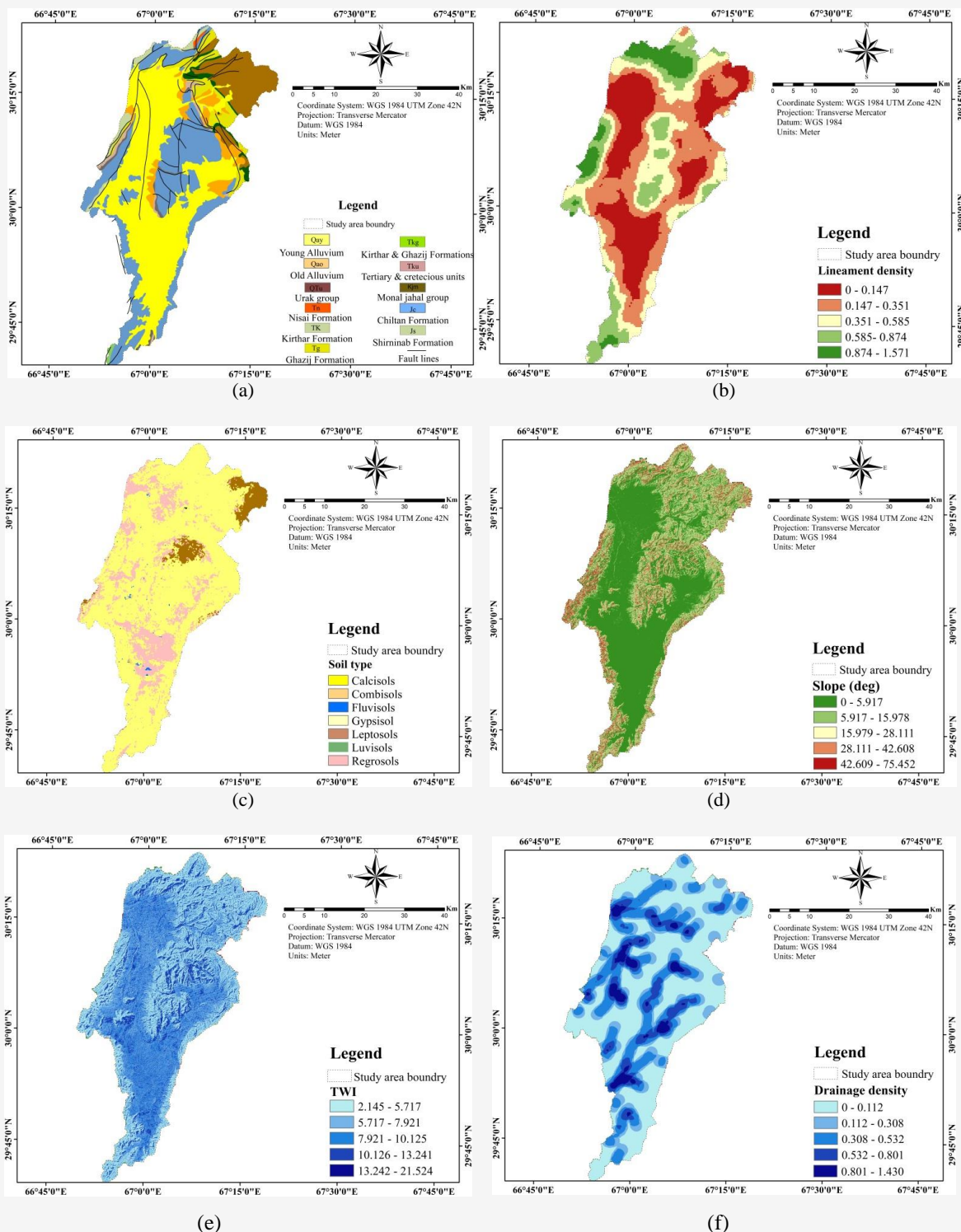


Figure 2: Thematic/factors maps
 (a) Geology (b) Lineament density (c) Soil type (d) Slope (e) TWI (f) Drainage density
 (continue next page)

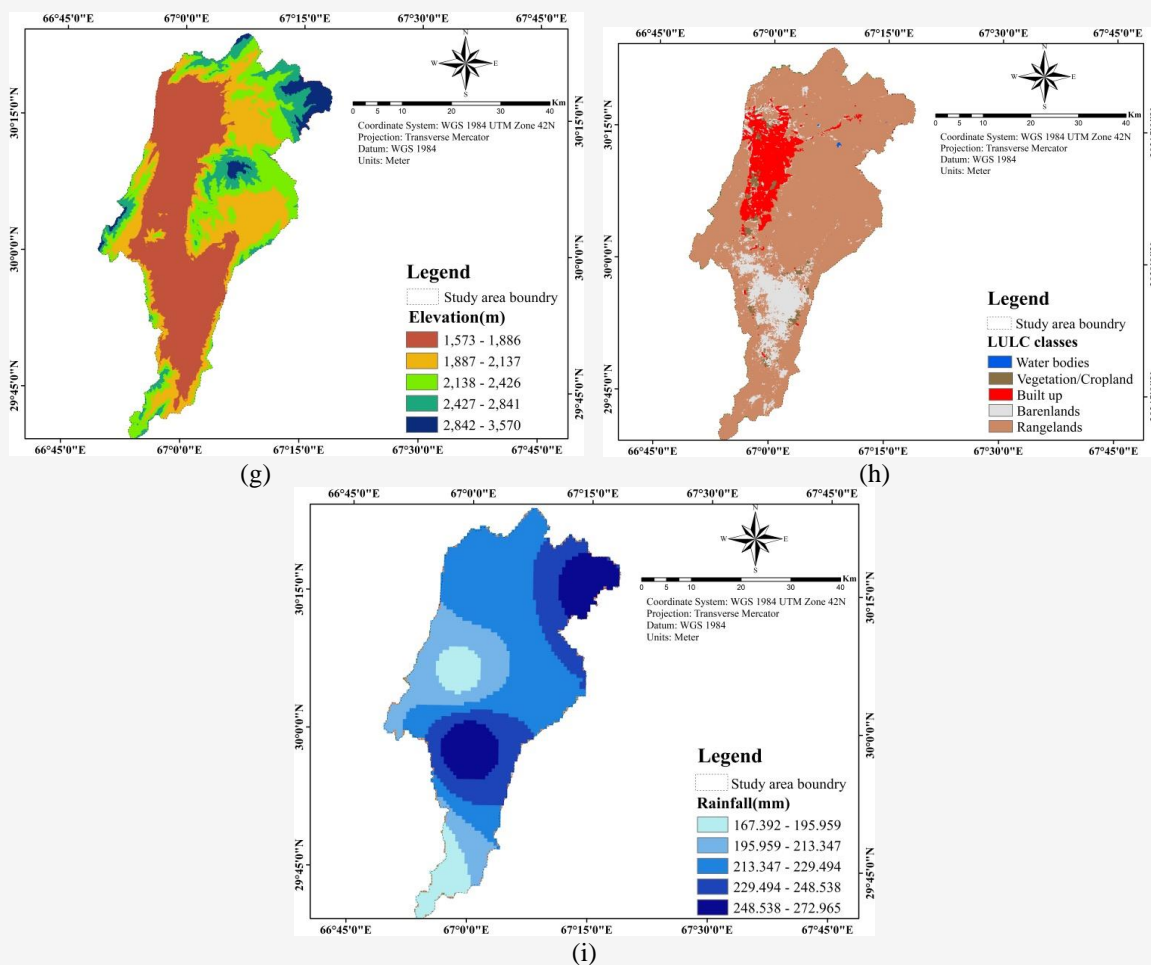


Figure 2: Thematic/factors maps

(g) Elevation (h) LULC (i) Rainfall (continue from previous page)

2.2.3 Soil types

The infiltration process is greatly influenced by the texture of the soil, which makes soil one of the main influencing factors in GW recharge studies [38]. The soil map was downloaded from International Soil Reference and Information Centre (ISRIC) website (<https://www.isric.org/>). The study area comprised seven types of soil namely; calcisols, combisols, fluvisols, gypsisols, leptosols, luvisols, and regosols (Figure 2(c)).

2.2.4 Slope

The slope represents the angle between the tangent plane and the horizontal plane at any given point [39]. The slope plays a crucial role in determining the flow formation process and infiltration rate [40]. Many of researchers reported an inverse relation between slope and infiltration rate [41][42] and [43]. Gentle slope areas have a high infiltration rate, so more suitable for GW recharge and vice versa [44].

The slope map of the study area was generated from DEM using the "Spatial Analysis Tools" in ArcGIS 10.8 (Figure 2(d)). The study area includes steep areas, with high slopes found in the northern and eastern sections due to the mountainous terrain, making slope a key factor in the current study.

2.2.5 Topographic Wetness Index (TWI)

TWI describes how topography affects hydrologic processes. It relates to GW flow movement and its retentions in subsurface zones [45]. TWI is computed as Equation 1:

$$TWI = \ln \left(\frac{\alpha}{\tan(\beta)} \right) \quad \text{Equation 1}$$

Where, α denotes Specific contributing area and β denotes Topographic slope of the area.

The areas with higher topographic wetness index (TWI) values are more suitable for GW recharge, as they indicate higher GW potential zones [46] and [47]. This is in contrast to areas with lower TWI values [48]. To achieve this, in ArcMap, we first projected the digital elevation model (DEM) to WGS84/UTM Zone 42 N. Then, we followed a series of steps including filling the DEM, determining the flow direction and accumulation, calculating the slope in degrees, calculating the radiance of slope, and scaling the flow accumulation. Finally, we determined the TWI using the natural logarithm of the scaled flow accumulation divided by the tangent of the slope (Figure 2(e)).

2.2.6 Drainage Density (DD)

Drainage density represents spatial distribution of the streams length per unit area [49][50] and [51]. Drainage density is one of the key factors in assessing and distribution of GW potentials over an area [52][53] and [54]. It describe the occurrence and flow pattern of water under the surface [50] and [55]. The DD has an inverse relationship with the permeability[56]. DD and surface runoff have a direct relationship with each other. In regions with low DD, infiltration is greater compared to regions with high DD[57] and good sources of high GW recharge [58]. The DD value is computed from the following as Equation 2 [59]:

$$DD = \frac{1}{A} \sum_{i=1}^n S_i$$

Equation 2

Where, S_i denotes the drainage length, i is the drainage order and A is the unit area in km^2 .

The Stream Network was generated using "Hydrology Tool" in ArcMap. The following steps were taken: Fill DEM => Flow Direction => Flow Accumulation => Stream Order => Stream to Feature => Line density (Figure 2(f)). The flow accumulation threshold dependent on area size. In current study flow accumulation was taken "flow accumulation > 5000" using map algebra.

2.2.7 Elevation

Altitude is a crucial factor in GW recharge as it triggers water flow under gravity [33] and [60]. Studies have indicated that the transfer of water from higher to lower altitudes is more pronounced in mountainous regions due to their elevated levels. Moreover, it has been established that flat surfaces are more effective in recharging water sources as compared to inclined surfaces and high-altitude

regions [44]. The study area consists mostly of mountainous regions with steep altitudes, leading altitude to be a critical factor that impacts groundwater recharge in the study (Figure 2(g)).

2.2.8 Land Use Land Cover (LULC)

The Land Use and Land Cover (LULC) is a crucial factor in determining appropriate locations for GW recharge [61]. For the purposes of our current study, we utilized a LULC map that was conveniently available for download from the Living Atlas by Esri. The exact website that we obtained the map from can be found at <https://livingatlas.arcgis.com/>. The study area having six classes; waterbody, trees, cropland, builtup, barrenland and rangeland (Figure 2(h)).

2.2.9 Rainfall

The characteristics of rainfall affect infiltration, runoff, and GW recharge [62] and [63]. The study has obtained rainfall data from the department of irrigation, Balochistan. The data covers the last 30 years (1980 to 2010), and the average rainfall data from multi-rain gauge stations were interpolated using the "Spatial Analyst Tools" > Interpolation > IDW. This process produced a rainfall contour map that was used to extract the rainfall map for the study area by applying the "Spatial Analyst Tool" > Extraction > Extract by Mask (Figure 2(i)).

2.3 Methodological Overview

The current study utilizes a multi-parameter dataset consisting of geology, lineament density, drainage density, soil type, slope, elevation, TWI, average rainfall, and LULC to identify GW recharge potential zones. The study employs three models - AHP, FAHP, and FR - to delineate these zones, providing a comprehensive understanding of the factors that contribute to GW recharge potential in the area. The methodological framework for this study is outlined in Figure 3. The mapping of the GW recharge zone is divided into four stages, as given below:

Stage 1: Data acquisition and database generation: In the initial stage, a thorough evaluation was conducted to identify nine key factors that impact GW recharge zones. Based on this evaluation, a comprehensive geospatial database was created, which forms the foundation for further analysis.

Stage 2: Preprocessing and the generation of thematic maps: The second stage included preprocessing of all acquired data and generating thematic maps from satellite and conventional data using the ArcGIS environment.

Stage 3: Weight assignment and reclassification of thematic layers: In the third stage of analysis, three models were employed to assign weights to different thematic maps based on their importance to GW recharge. These maps were then divided into three distinct classes, which corresponded to high, moderate, and low recharge zones. To produce final maps of GW recharge potential, various techniques such as AHP-Weighted overlay, AHP-Weighted sum, fuzzy-AHP overlay, and FR-based models were used in ArcGIS. By merging all the layers, the final maps were created.

Stage 4: Results validation: In the fourth and final stage, the results were validated to ensure their accuracy. This was done through the use of receiver operating characteristics (ROC) curves for each of the models. An area under the receiver operating characteristic (AUC) curve was generated to visually represent the correlation between the accumulated percentage of water wells and the delineation of different groundwater potential recharge zones. Additionally, the electrical conductivity (EC) of wells was also used for cross-validation. The final results have been verified using these methods.

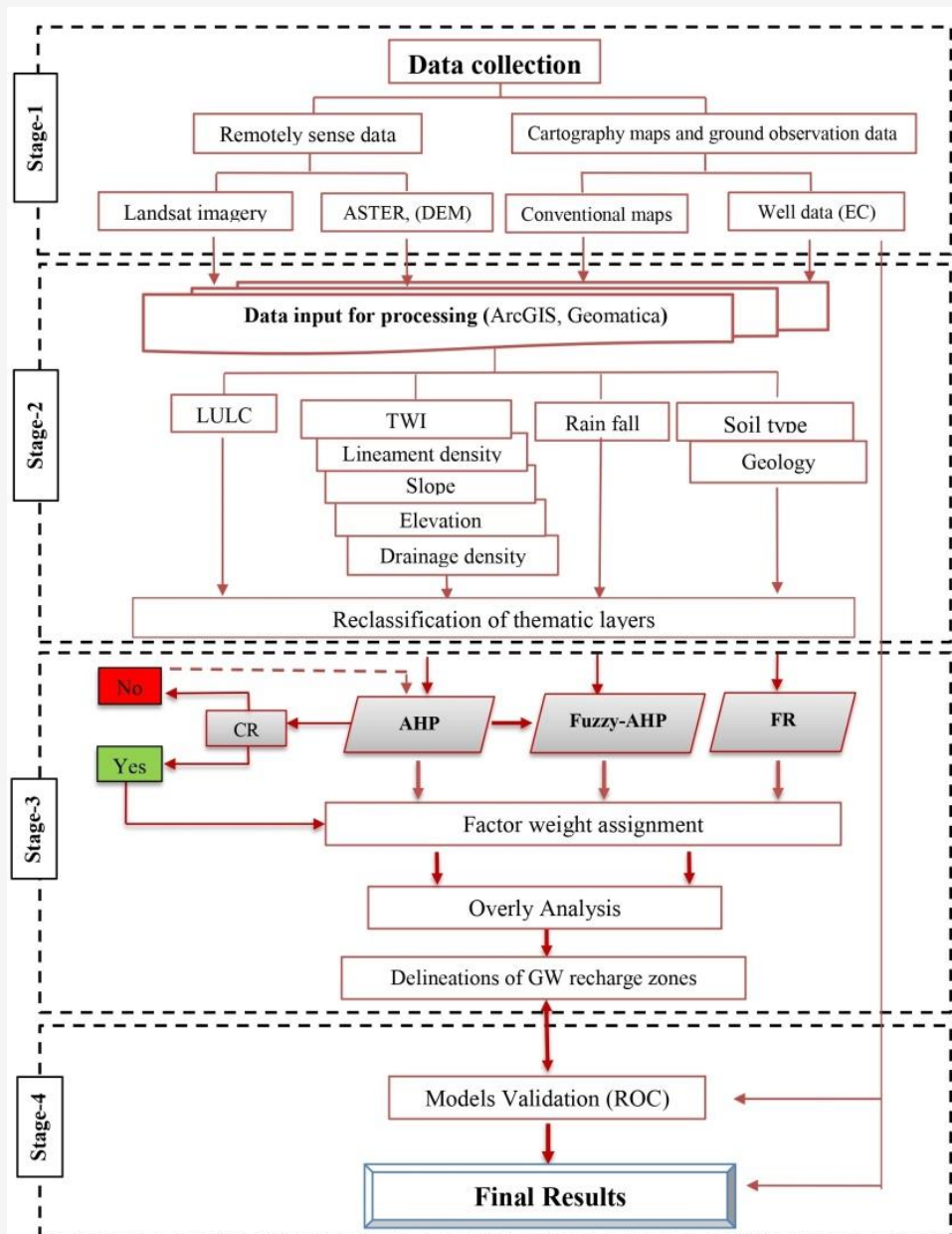


Figure 3: Methodological flowchart of the current study

3. Results and Discussions

3.1 AHP Model-Based Weight Assignment

Thomas Saaty developed the Analytic Hierarchy Process (AHP) at the Wharton School of Business in 1980. It offers decision-makers a method to analyze and address intricate issues within a hierarchical framework. It clearly displays the relationships among goals, objectives, sub-objectives, and alternatives [30]. The AHP method was used in ArcGIS to determine the Normalized Principal Eigenvector (NPEV) or Percent Weight in the weighted overlay Analysis. The process involves entering contributing criteria based on their importance in mapping GW recharge zones. Factors are given scores between 1-9, indicating their relative importance in pairwise comparisons [64]. A pairwise comparison matrix (PCM) was constructed based on saaty scale and expert opinion (shown in Table 1).

Where, GE represents geology, ST represents soil type, SL represents slope, LULC represents land use/land cover, LD denotes lineament density, EL denotes elevation, DD denotes drainage density, TWI represents topographic wetness index and RF represents rainfall. Once the Pairwise comparison matrix was created, normalized weights (W_n) were computed (Table 2) in the following manner Equation 3 [65]:

$$W_n = \frac{GM_n}{\sum_{n=1}^{Nf} GM_n}$$

Equation 3

Where, GM_n designates the geometric mean of n^{th} rows elements.

Finally Normalized weights (w_n) were verified using consistency ratio matrix [64]. A Consistency Ratio (CR) is the ratio of the Consistency Index (CI) to the Random Consistency Index. (RI). The value of CI for GW potential and recharge zone parameters investigated in this study was calculated as Equation 4.

$$CI = \frac{\lambda_{\max} - n}{n - 1}$$

Equation 4

Where, n represents the quantity of criteria and λ_{\max} stands for the Principal Eigenvalue value (Ratio of weight sum to the criteria weight) obtained from consistency ratio matrix (Table 4). The Random index (RI) was derived from Table 3 of [64], which depends on number of criteria (n) adopted in the study. The CR value is utilized to evaluate the consistency of the matrix. The CR value must be determined less than 0.1 [64] and [66]. If the value of CR is less than or equal to 0.1(10%), the inconsistency is acceptable.

Table 1: Analytic hierarchy process pairwise comparison matrix (PCM)

PCM	GE	ST	SL	LULC	LD	EL	TWI	DD	RF
GE	1	1	2	3	3	3	5	5	5
ST	1	1	1	2	3	3	5	5	5
SL	0.50	1	1	2	3	3	4	5	5
LULC	0.33	0.50	0.50	1	2	3	5	5	4
LD	0.33	0.33	0.33	0.50	1	1	3	4	2
EL	0.33	0.33	0.33	0.33	1	1	3	3	3
TWI	0.20	0.20	0.25	0.20	0.33	0.33	1	1	1
DD	0.20	0.20	0.20	0.20	0.25	0.33	1	1	1
RF	0.20	0.20	0.20	0.25	0.50	0.33	1	1	1
Sum	4.10	4.77	5.82	9.48	14.08	15.00	28.00	30.00	27.00

Table 2: Normalized relative weight (W_n), and Normalized Principal Eigen Vector (NPEV)

NPCM	GE	ST	SL	LULC	LD	EL	TWI	DD	RF	Eigen Vector	NPEV (%)
GE	0.244	0.210	0.344	0.316	0.213	0.200	0.179	0.167	0.185	0.229	22.9
ST	0.244	0.210	0.172	0.211	0.213	0.200	0.179	0.167	0.185	0.198	19.8
SL	0.122	0.210	0.172	0.211	0.213	0.200	0.143	0.167	0.185	0.180	18.0
LULC	0.081	0.105	0.086	0.105	0.142	0.200	0.179	0.167	0.148	0.135	13.5
LD	0.081	0.070	0.057	0.053	0.071	0.067	0.107	0.133	0.074	0.079	7.9
EL	0.081	0.070	0.057	0.035	0.071	0.067	0.107	0.100	0.111	0.078	7.8
TWI	0.049	0.042	0.043	0.021	0.024	0.022	0.036	0.033	0.037	0.034	3.4
DD	0.049	0.042	0.034	0.021	0.018	0.022	0.036	0.033	0.037	0.032	3.2
RF	0.049	0.042	0.034	0.026	0.036	0.022	0.036	0.033	0.037	0.035	3.5
Sum	1	1	1	1	1	1	1	1	1	1	100.0

Table 3: Random Index (RI) value related to the number of criteria (n) [64]

n	1	2	3	4	5	6	7	8	9	10
RI	0	0	0.58	0.9	1.12	1.24	1.32	1.41	1.45	1.49

Table 4: Consistency ratio matrix

Matrix	GE	ST	SL	LULC	LD	EL	TWI	DD	RF	Weight	λ_{max}
GE	0.229	0.198	0.361	0.404	0.238	0.233	0.170	0.162	0.175	2.170	9.494
ST	0.229	0.198	0.180	0.270	0.238	0.233	0.170	0.162	0.175	1.855	9.380
SL	0.114	0.198	0.180	0.270	0.238	0.233	0.136	0.162	0.175	1.707	9.469
LULC	0.076	0.099	0.090	0.135	0.159	0.233	0.170	0.162	0.140	1.265	9.383
LD	0.076	0.066	0.060	0.067	0.079	0.078	0.102	0.130	0.070	0.729	9.194
EL	0.076	0.066	0.060	0.045	0.079	0.078	0.102	0.097	0.105	0.709	9.120
TWI	0.046	0.040	0.045	0.027	0.026	0.026	0.034	0.032	0.035	0.311	9.130
DD	0.046	0.040	0.036	0.027	0.020	0.026	0.034	0.032	0.035	0.296	9.103
RF	0.046	0.040	0.036	0.034	0.040	0.026	0.034	0.032	0.035	0.322	9.196

Table 5: Thematic layer rank and weight in terms of GW recharge perspective

Thematic Layer	Features Classes	GWR Perspective	Rank Assigned	Weight (%)
Geology	Tg/ KJm/ TKu/ Tk/ Tkg/ Tn/Js	Low	1	23
	QTu/Jc	Moderate	2	
	Qay/Qao	High	3	
Soil Type	Gypsisols/ Regosols	Low	1	20
	Luvisol/ Combisols	Moderate	2	
	Calcisols/ Fluvisols/ Leptosols	High	3	
Slope (degree)	29.88 - 75.45	Low	1	18
	10.35 - 29.88	Moderate	2	
	0-10.35	High	3	
LULC	Built Up/ Bare land/ Rangeland	Low	1	13
	Waterbodies/ Trees/ CropLand	High	3	
Lineament Density	0 - 0.308	Low	1	8
	0.308 - 0.696	Moderate	2	
	0.696 - 1.571	High	3	
Elevation (m)	488.93 - 3569.53	Low	1	8
	1987.789 - 2488.9	Moderate	2	
	1572.776 - 1987.7	High	3	
TWI	2.1459 - 6.384	Low	1	3
	6.384 - 9.715	Moderate	2	
	9.715 - 21.523	High	3	
Drainage Density (km/km ²)	0.560 - 1.429	Low	1	3
	0.196 - 0.560	Moderate	2	
	0 - 0.196	High	3	
Rainfall (mm)	167.392 - 209.207	Low	1	4
	209.207 - 237.360	Moderate	2	
	237.360 - 272.965	High	3	

However, if the CR value is higher than 0.1(10%), then the comparison judgment must be re-evaluated. In the present study the λ_{max} value obtained is 9.274 (from Table 4) and RI is 1.45 (from Table 3). The value of $CR=0.023 < 0.10$, which suggest that the inconsistency is acceptable for these 9 parameters under consideration in current study.

Before applying weighted overlay analysis, the ranks were assigned to each factor of all thematic layers, and the weight was assigned according to their relative importance to GW recharge potential

(Table 5) using the Analytic Hierarchical Process (AHP) technique [67]. After assigning weights to all thematic layers, ranks/scale values from 1 to 3 were given for the sub variable of every thematic layer, in line with their importance for GW recharge potential occurrence. According to this study, 1 represents less vital (low recharge zones), and 3 represents more vital (high recharge) for GW recharge potential zoning. Final weighted overlay was calculated (shown in Figure 5(a)). In weighted sum, all classified thematic were multiplied with

their corresponding weights and sum in the "weighted sum" tool in overlay analysis (shown in Figure 5(b)).

3.2 FAHP Model-Based Weight Assignment

The Fuzzy-Analytic Hierarchy Process (FAHP) is a decision-making model that combines the AHP method with fuzzy logic theory. This hybrid model is designed to handle uncertainty and vagueness in the decision-making process. In simpler terms, fuzzy logic theory is used to apply the theory of fuzzy sets in decision-making [68]. The fuzzy set theory is a mathematical framework for dealing with uncertainty and vagueness in data by allowing partial membership in a set [69]. Fuzzy set values range from 0 to 1, indicating gradual class transition [70]. Fuzzy-AHP was used to upgrade the AHP analysis by introducing fuzzy weight. The analysis involved two stages. The first stage included calculating the weights of the thematic layers. This was achieved by constructing pairwise-comparison matrices for each the criterion in the decision process and then upgrading them using triangular fuzzy numbers (TFNs). The TFNs are represented by *l* (lowest possible value), *m* (most likely possible value), and *u* (highest possible value) (shown in Tables 6 and 7). In the second step the geometric mean and the fuzzy weights for the thematic layers were calculated by employing Buckley's geometric mean Equations (5 and 6) [71]:

$$R_i = (a_{i1} \otimes a_{i2} \otimes \dots \otimes a_{in})^{1/n} \quad \text{Equation 5}$$

$$W_i = R_i \otimes (R_1 \otimes R_2 \otimes \dots \otimes R_n)^{-1} \quad \text{Equation 6}$$

Where R_i denotes the geometric mean values of criterion *i* to each criterion and a_{in} is fuzzy comparisons value of criterion *i* to criterion *n*; W_i denotes the fuzzy weight of the *i*th criterion [70].

The Fuzzy weights were later standardized in order to determine the weight of each criteria utilizing Equation 7 [72]:

$$N_i = \frac{M_i}{\sum_{i=1}^n M_i} \quad \text{Equation 7}$$

Where $M_i = (lwi + mwi + uwi)/3$, $N_i = 1$, $i = 1, 2, \dots, n$ and *lwi*, *mwi*, *uwi* represents the lower, middle, and upper values of the fuzzy weights of the *i*th criterion, respectively.

In the second phase of the analysis, fuzzy membership values were allocated to each thematic layer. The ArcGIS platform was utilized to assign the fuzzy membership values by employing the linear transformation function. The fuzzy linear transformation is a frequently utilized technique in research related to GW recharge [73]. After the linear transformation of classified maps, normalized fuzzy weights were multiplied with each thematic map using a raster calculator in the spatial analyst tool. Finally, fuzzy overlay was employed to get the final GW recharge zones map. The Final map was reclassified into three GW recharge potential zones viz. high, moderate, and low recharge zones (shown in Figure 5(c)).

Table 6: Fuzzy pairwise comparison matrices (FPCM)

FPCM	GE	ST	SL	LULC	LD	EL	TWI	DD	RF
GE	(1,1,1)	(1,1,1)	(1,2,3)	(2,3,4)	(2,3,4)	(2,3,4)	(4,5,6)	(4,5,6)	(4,5,6)
ST	(1,1,1)	(1,1,1)	(1,1,1)	(1,2,3)	(2,3,4)	(2,3,4)	(4,5,6)	(4,5,6)	(4,5,6)
SL	(0.33,0.50,1.00)	(1,1,1)	(1,1,1)	(1,2,3)	(2,3,4)	(2,3,4)	(3,4,5)	(4,5,6)	(4,5,6)
LULC	(0.25,0.33,0.50)	(0.33,0.50,1.00)	(0.33,0.50,1.00)	(1,1,1)	(1,2,3)	(2,3,4)	(4,5,6)	(4,5,6)	(3,4,5)
LD	(0.25,0.33,0.50)	(0.25,0.33,0.50)	(0.25,0.33,0.50)	(0.33,0.50,1.00)	(1,1,1)	(1,1,1)	(2,3,4)	(3,4,5)	(1,2,3)
EL	(0.25,0.33,0.50)	(0.25,0.33,0.50)	(0.25,0.33,0.50)	(0.25,0.33,0.50)	(1,1,1)	(1,1,1)	(2,3,4)	(2,3,4)	(2,3,4)
TWI	(0.17,0.20,0.25)	(0.17,0.20,0.25)	(0.20,0.25,0.33)	(0.17,0.20,0.25)	(0.25,0.33,0.50)	(0.25,0.33,0.50)	(1,1,1)	(1,1,1)	(1,1,1)
DD	(0.17,0.20,0.25)	(0.17,0.20,0.25)	(0.17,0.20,0.25)	(0.17,0.20,0.25)	(0.20,0.25,0.33)	(0.25,0.33,0.50)	(1,1,1)	(1,1,1)	(1,1,1)
RF	(0.17,0.20,0.25)	(0.17,0.20,0.25)	(0.17,0.20,0.25)	(0.20,0.25,0.33)	(0.33,0.50,1.00)	(0.25,0.33,0.50)	(1,1,1)	(1,1,1)	(1,1,1)

Table 7: Fuzzy-geometric mean (R_i), fuzzy-weight (W_i), and normalized weight (N_i) of each criterion

	Fuzzy Geometric Mean			M_i			Fuzzy Weight (W_i)	Normalized Weight (N_i)
	(R_i)			l	m	u		
GE	2.00	2.66	3.26	0.134	0.228	0.365	0.242	0.217
ST	1.85	2.36	2.79	0.124	0.202	0.312	0.213	0.191
SL	1.59	2.13	2.74	0.107	0.182	0.306	0.198	0.178
LULC	1.12	1.54	2.17	0.075	0.132	0.243	0.150	0.135
LD	0.68	0.91	1.25	0.045	0.078	0.140	0.088	0.079
EL	0.68	0.89	1.17	0.045	0.075	0.130	0.084	0.075
TWI	0.34	0.39	0.48	0.022	0.033	0.053	0.036	0.033
DD	0.32	0.37	0.44	0.112	0.031	0.049	0.064	0.058
RF	0.35	0.41	0.52	0.023	0.035	0.057	0.038	0.035

Table 8: Frequency ratio values for each thematic layer and its classes

Thematic Layers	Assigned Rank	Number of Pixels in Domain	Percentage of Domain	Number of Wells	Percentage of Wells	FR
GE	1	248,378	11.98	5	6.67	0.56
	2	821,228	39.61	4	5.33	0.45
	3	1,003,759	48.41	66	88.00	7.35
LD	1	1,119,729	53.96	63	84.00	1.56
	2	682,608	32.90	11	14.67	0.27
	3	272,740	13.14	1	1.33	0.02
DD	1	256,820	12.39	15	20.00	1.61
	2	675,677	32.59	22	29.33	2.37
	3	1,140,980	55.03	38	50.67	4.09
RF	1	615,263	29.68	28	37.33	1.26
	2	941,832	45.43	47	62.67	2.11
	3	516,018	24.89	0	00.00	0.00
ST	1	369,915	17.84	11	14.67	0.82
	2	7,726	0.37	0	0.00	0.00
	3	1,696,393	81.79	64	85.33	1.04
SL	1	209,427	10.18	4	5.33	0.52
	2	425,130	20.67	1	1.33	0.13
	3	1,422,180	69.15	70	93.33	9.17
TWI	1	736,991	35.83	12	16.00	0.45
	2	802,555	39.02	9	12.00	0.31
	3	517,191	25.15	54	72.00	2.86
EL	1	219,230	10.57	1	1.33	0.13
	2	795,597	38.37	1	1.33	0.13
	3	1,058,650	51.06	73	97.33	9.21
LULC	1	2,040,414	98.42	75	100.00	1.02
	3	32,831	1.58	0	0.00	0.00

3.3 FR Model-Based Weight Assignment

The FR model is a statistical model that can be used to assess the relationship between independent and dependent variables in geospatial analysis. This model is bi-variate and provides a convenient way to define the probability of this relationship. Additionally, the FR model can be applied to multi-classified maps, making it a versatile tool for geospatial analysis [74]. Many researchers have successfully applied FR models for GW recharge mapping [65][75][76][77] and [78]. The structural composition of the FR model relies heavily on the correlations and observed relationships between each groundwater conditioning factor and the distribution of well locations. The FR value attributed to each class of groundwater-related factors can be effectively expressed via the utilization of Equation 8:

$$FR = \frac{WT}{GM} \quad \text{Equation 8}$$

Where W denotes the count of pixels with GW wells and G represent the total number of GW wells within the study area. M represents the number of pixels within the class area of the factor, while T represents the total count of pixels within the study area. In a given pixel, GW recharge potential can be determined according to the Equation 9 [79]:

$$GRPZ = \sum_{i=1}^n FR_i \quad \text{Equation 9}$$

Where GRPZ represents the GW recharge potentials zones and FR_i is the FR value of each factor. In comparison to AHP and FAHP, in FR technique, the

weight to each class is not assigned on the bases of properties of the influencing factors but given on the bases of spatial occurrence of the wells in each class. Similarly, the FR is calculated for all the conditioning factors (Table 8). Finally, the GW recharge zones map has been created by using raster calculator in ArcGIS environment (shown in Figure 5(d))

3.4 Thematic Layers Reclassification According to GW Rechargeability

3.4.1 Geology and reclassified geology layer

Lithology refers to the physical characteristics of rocks, including mineral composition and grain size [34]. Lithology controls the infiltration and flow processes of GW [35] and [36]. The study area is mostly covered by young alluvium (Qay), which makes up 46% of the area, followed by Chiltan formation (Jc) at 29.8%, Urak formation (QTu) at 8%, old alluvium (Qao) at 5.2%, Ghazij formation (Tg) at 4.5%, Shirinab formation (Js) at 2.4%, kirthar formation (Tk) at 1.4%, Tertiary and cretaceous (Tku) at 1.3%, Monal jahal formation (Kjm) at 1% and Nasai formation (Tn) at 0.2%. The major lithologies exposed in wide areas are limestone, conglomerates, and sandstone. Geology was reclassified into three recharge potential classes based on permeability and porosity: low (Tg/KJm/TKu/Tk/Tkg/Tn/Js), moderate (QTu/Jc), and high (Qay/Qao) (Figure 4(a)).

3.4.2 Lineament density and reclassified lineament density layer

Lineaments are critical geological features that act as reservoirs and conduits for minerals and hydrocarbons and reveal local and regional tectonic behavior [37]. The Chaman Fault's tectonic movements have caused the formation of various folding, faulting, fractures and joint systems in the limestone formations of the area. These fractured zones and joint systems show promise for the occurrence and movement of GW. The lineaments may lead to the development of secondary porosity and permeability in rocks [34] and [39]. Therefore, high lineament density areas are likely to have significant potentials for GW recharge. First Lineaments density map was classified using natural breaks (Jenks) into three classes and then reclassified lineaments according to GW recharge zoning i.e. Low (0-0.308), moderate (0.308-0.696), and high (0.696 - 1.571) (Figure 4(b)).

3.4.3 Soil types and reclassified soil types layer

The area under study consists of seven distinct soil types: Calcisols, cambisols, fluvisols, gypsisols, leptosols, luvisols, and regosols. Calcisols are the most prevalent soil type, covering 1347.64km² of the study area. Regosols cover nearly 300km², while leptosols cover 88.36 km², cambisols cover 5.5 km², fluvisols cover 3 km², gypsisols cover 0.65km², and luvisols cover an area of 0.1 km². (<https://soilgrids.org/>). The classification of the soils was revised based on their grain size and the proportion of sand, clay, and silt in them. (<https://www.isric.org/>). Coarse-grained soils are known for their ability to infiltrate water at a high rate and are given high recharge potential values [80] and [81]. The reclassified soil type map shows leptosols, fluvisol, and calcisol characterize the high recharge areas because they are coarse-grained and have high sand contents [82]. Moderate value is assigned to cambisols and luvisols due to their ability to hold water well and good internal drainage [83]. Regosols and gypsisol have mostly high clay and fine texture [83], therefore assigned low recharge potentiality (Figure 4(c)).

3.4.4 Slope and reclassified slope layer

Slope has an inverse relation between infiltration rates [41] [42] and [43]. The areas with gentle slopes have high infiltration rate, so more suitable to GW recharge and vice versa [40] and [44]. In the mountainous region high slope is the main impediment in GW recharge whereas low slopes are favorable for GW recharge. Accordingly slope map was reclassified using natural breaks (Jenks) into three classes and then reclassified according to GW rechargeability; Low (2.145- 6.384), moderate (6.384 - 9.715), and high (9.715 - 21.523) GW recharge zones (Figure 4(d)).

3.4.5 TWI and reclassified TWI layer

TWI describes the impact of topography on hydrologic processes. It relates GW flow movement and its retentions in subsurface zones [45]. There is a positive correlation between TWI and GW recharge potentials. Higher TWI values shows a higher GW potential zones so areas with higher TWI are more suitable for GW recharge as compared to area with low TWI values [46][47] and [48]. TWI map was classified using natural breaks (Jenks) into three classes then reclassified according to GW rechargeability; Low (2.145 - 6.384), moderate (6.384 - 9.715), and high (9.715 - 21.523) GW recharge zone (Figure 4(e)).

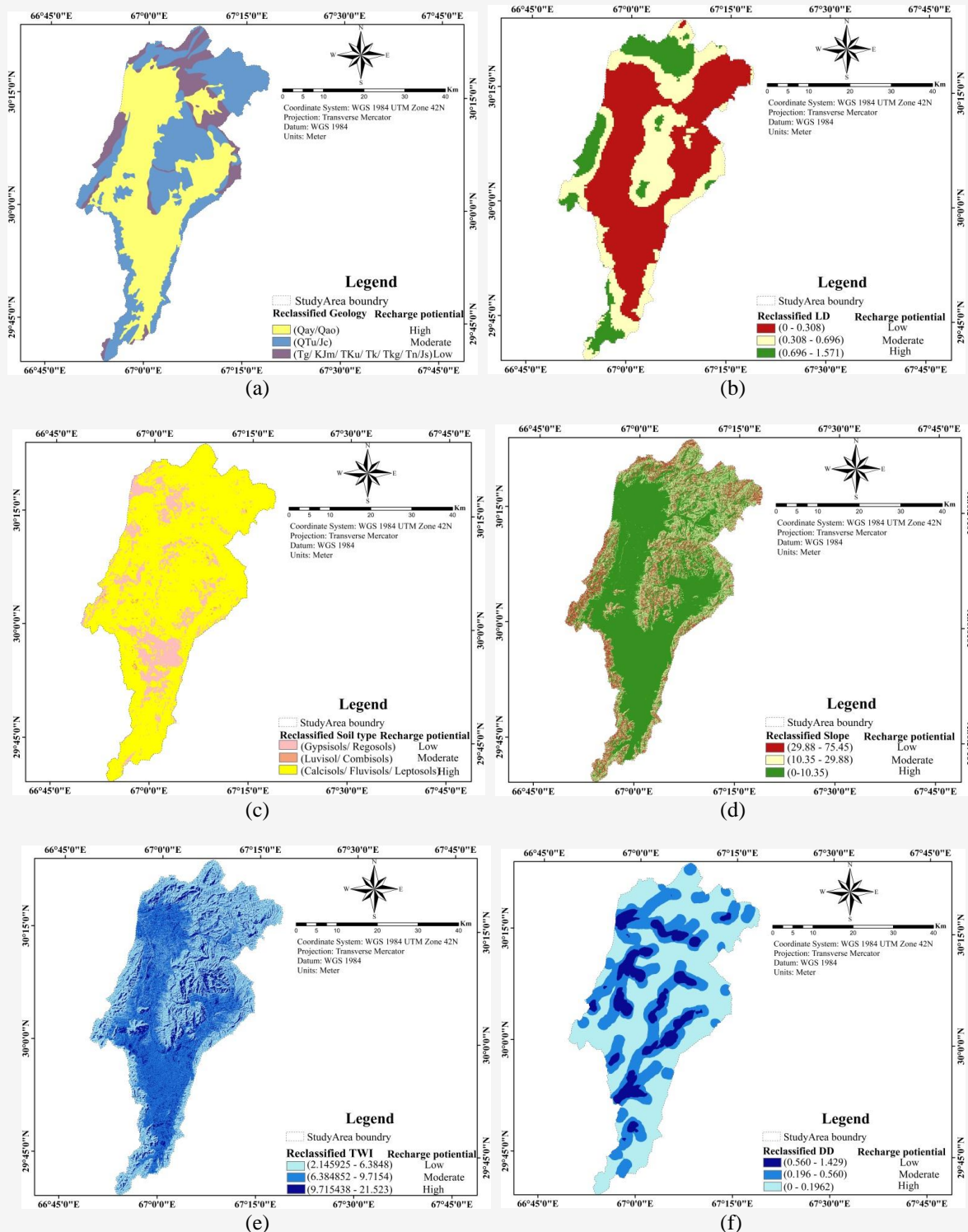


Figure 4: Reclassified layers
 (a) Geology (b) Lineament density (c) Soil type (d) Slope (e) TWI (f) Drainage density
 (continue next page)

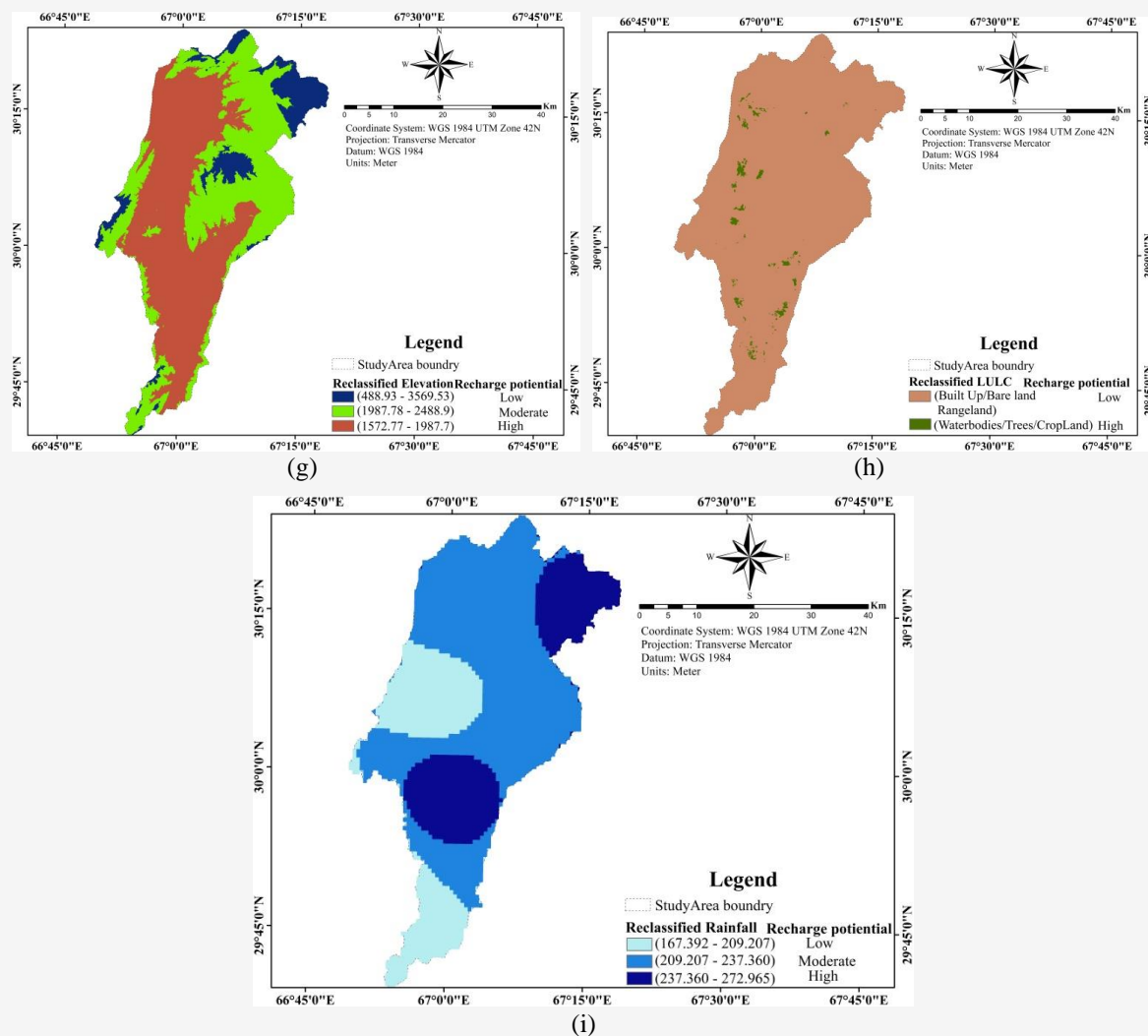


Figure 4: Reclassified layers
(g) Elevation (h) LULC and (i) Rainfall
(continue from previous page)

3.4.6 Drainage density & reclassified drainage density layer

The Drainage density is a crucial factor in the assessment and distribution of GW potentials in an area [52] [53] and [54]. In terms of GW recharge, low drainage density implies more infiltration [57] and good sources of high GW recharge potentials [58]. Accordingly, Low drainage density areas were given more importance than high drainage density areas, as illustrated in Figure 4(f). The drainage density map has been classified using natural breaks (Jenks) into three classes, then reclassified according to GW rechargeability; as low (0.560 - 1.429), moderate (0.196 - 0.560) and high (0 - 0.196), recharge zones.

3.4.7 Elevation and reclassified elevation layer

International Journal of Geoinformatics, Vol. 20, No. 7, July, 2024

ISSN: 1686-6576 (Printed) | ISSN 2673-0014 (Online) | © Geoinformatics International

The study area comprised of mountainous regions having high elevations. Based on GW rechargeability, elevation has been classified using natural breaks (Jenks) into three classes, then reclassified according to GW rechargeability; Low (488.93 - 3569.53), moderate (1987.789 - 2488.9), and high (1572.776 - 1987.7). The recharge potential of flat surfaces is greater than that of inclined surfaces and higher elevations, resulting in a higher rank being assigned to lower elevations [44] (Figure 4(g)).

3.4.8 LULC and reclassified LULC layer

The LULC is an important indicator that helps in identifying suitable locations for GW (GW) recharge [61]. LULC comprised of areal distribution of vegetation cover, cropland and residential or built up. The study area has six classes; waterbody, trees,

cropland, builtup, barrenland and rangeland (Figure 2(h)). According to GW recharge perspective the LULC has been classified into two classes [50] and [84] (Figure 4(h)). The vegetation cover, waterbody and cropland assigned high weight as it has high GW infiltration [85], while builtup, barrenland and rangeland assigned low weight because of having high run-off and low infiltration rate [86].

3.4.9 Rainfall and reclassified rainfall layer

The study area falls in semiarid-arid region receiving average rainfall of 180-250mm/annul. The province is affected by two different meteorological systems (Western disturbances and Monsoon). In extreme cases oceanic currents and monsoon currents originating from the Arabian Sea can also reach southern part of the watershed and cause significant rainfall. In the north Western disturbances are the major cause of rainfall. Western disturbances are predominant in northern areas and high rainfalls occur. Monsoon is predominant more in southern parts. The generated rainfall map has been reclassified using natural breaks (Jenks) into three classes then reclassified according to GW rechargeability; low (167.392 - 209.207), moderate (209.207 - 237.360) and high (237.360 - 272.965), recharge potential zones (Figure 4(i)).

3.5 Final GW Recharge Potential Zones Mapping in ArcGIS Environment

Prior to the overlay analysis, all thematic layers underwent projection using WGS84/UTM Zone 42 N datum coordinate system. This was carried out to ensure a uniform resolution of 29*29m for optimal utilization within the ArcGIS environment. The GW recharge maps were created by overlaying all reclassified thematic layers (Geology, Soil type, Slope, LULC, Elevation, Lineament density, Drainage density, TWI, Rainfall) in the ArcGIS environment, as illustrated in Figure 4(a)-(i). To determine the final weight for each thematic layer, we used the analytical hierarchy process (AHP), integrated Fuzzy analytical hierarchy process (FAHP), and Frequency ratio models, which are outlined in Tables 5, 6, 7 and 8. The resulting maps

were then divided into three descriptive zones based on the recharge zone, namely "Low," "Moderate," and "High," each represented by distinct colors, as shown in Figures 5(a)-(d).

Table 9 displays the statistical and spatial distribution of each model (Figure 5(a)-(d)). The results of the AHP model-I show that 1449 km² (84%) of the study area falls under the moderate GW recharge zone, 254 km² (15%) falls under the high recharge zone, and 19 km² (1%) falls under the low recharge zone. On the other hand, the AHP model-II indicates that 321 km² (19%) of the area falls under the low recharge zone, 721 km² (42%) falls under the moderate zone, and 680 km² (39%) falls under the high recharge zone. Similarly, the FAHP model reveals that 269 km² (16%) of the region falls under the low zone, 718 km² (42%) falls under the moderate zone, and 736 km² (43%) falls under the high recharge zone. Finally, the FR model statistics show that 391 km² (23%) of the area falls under the low zone, 610 km² (35%) falls under the moderate zone, and 721 km² (42%) of the study area falls under the high recharge zone.

4. Results Validation with AUC and Well Data

The Receiver operating characteristic curve (ROC) and area under the curve (AUC) are used to predict classification accuracy [31] and [87]. Many of the researchers [31][65][69][72] and [88] have used ROC for validation of their research. In the current study, resultant maps of GW recharge potential zone, developed by GIS-based models (AHP, FAHP, FR) have been validated through the ROC curve. The AUC was plotted between the accumulated percentage of water wells and different GW recharge potential zones. AHP model-I (weighted overlay), AHP model-II (weighted sum), FAHP, and FR models showed 84%, 89%, 88%, and 81% prediction accuracy respectively (Figure 6). Since all these results fall in (0.8-0.9) very good class [89], hence applications of all models (AHP, FAHP, FR) showed very good accuracy in spatial prediction of GW recharge zone mapping, but AHP model-II showed more effectiveness than FAHP and FR in the current study.

Table 9: Spatial/Areal distribution of GW recharge zone

Models	AHP Model-I		AHP Model-II		FAHP Model		FR Model	
Area	(Km ²)	(%)	(Km ²)	(%)	(Km ²)	(%)	(Km ²)	(%)
Low	18.53	1.08	321.09	18.64	268.54	15.59	391.04	22.71
Moderate	1449.28	84.15	721.31	41.88	717.93	41.69	609.73	35.40
High	254.40	14.77	679.81	39.47	735.75	42.72	721.45	41.89

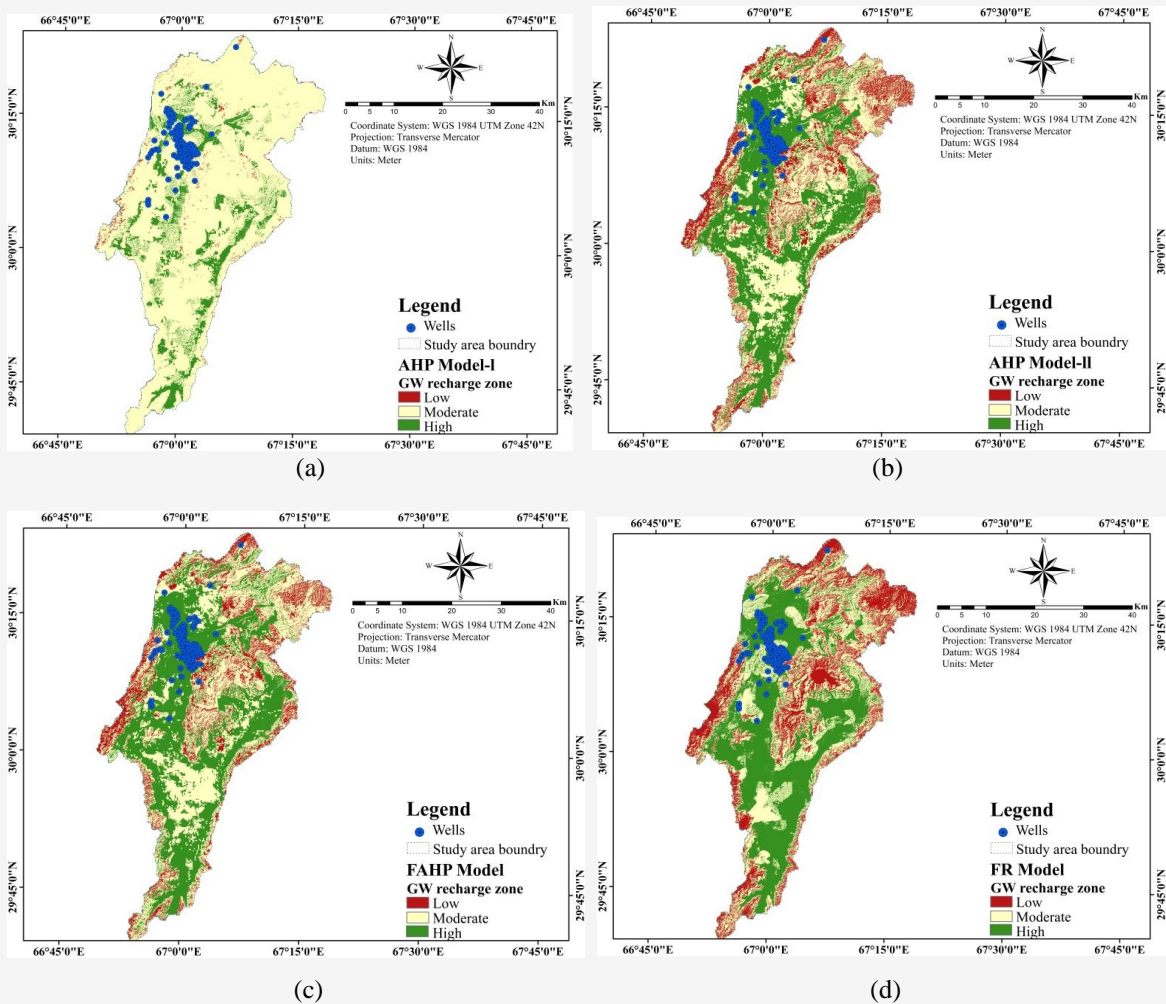


Figure 5: GW recharge zone maps using (a) AHP Model-I(WLC) (b) AHP Model-II(Wsum) (c) FAHP Model and (d) FR Model

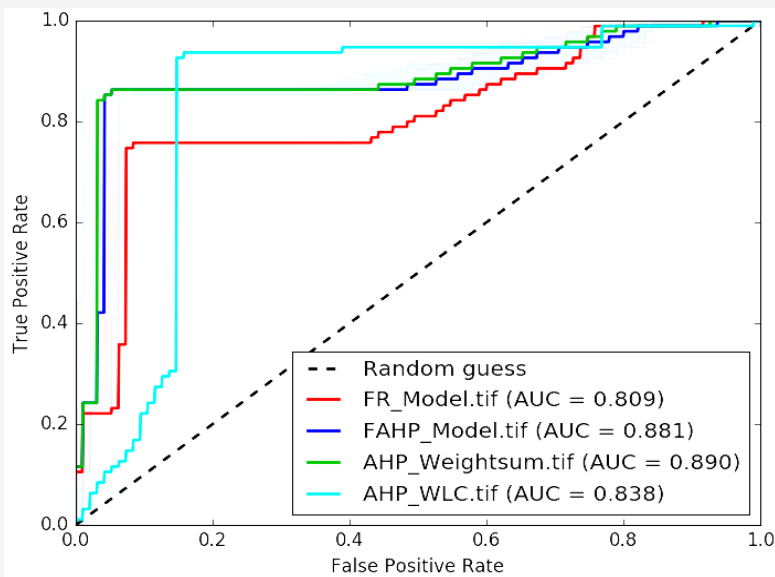


Figure 6: Receiver operating characteristics (ROC) curves for AHP, FAHP and FR models

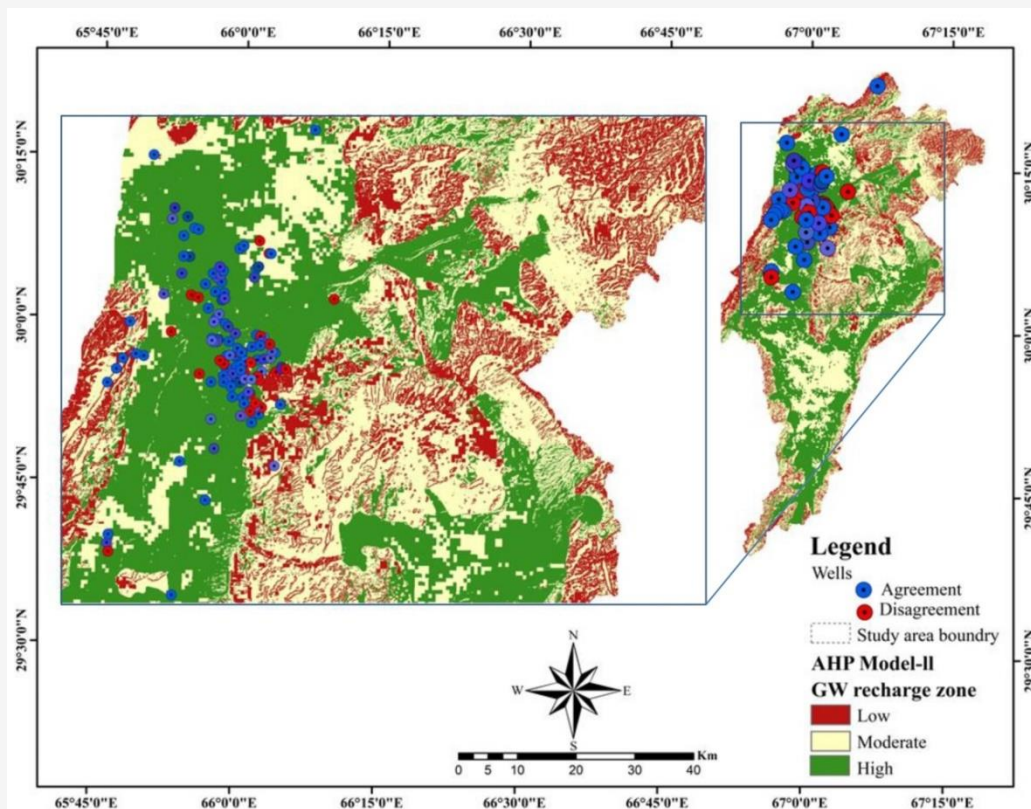


Figure 7: Showing validation (agreement/Disagreement) of wells on bases of EC

For cross-validation electrical Conductivity (EC) of well distributed over study was used to verify the GW recharge areas. Many researchers [69][72][90] and [91] used EC to verify demarcated GW recharge zones. The concentration of salt in GW is measured by EC, which reflects the level of ionic concentration in GW [69]. Based on EC readings, GW can be classified into three types. Type-1 GW has EC less than 1500 $\mu\text{S}/\text{cm}$ and is fresh-water with a low concentration of salts. Type-2 GW has EC between 1500-3000 $\mu\text{S}/\text{cm}$, indicating a moderate concentration of salts. Type-3 GW has EC greater than 3000 $\mu\text{S}/\text{cm}$, indicating high salinity [92] and [93]. In the current analysis 141 wells data, acquired from the Pakistan Council of Research in Water Resources (PCRWR) report, were used. EC range 300-1401 in study area. Based on EC, wells were divided into two types viz, type-1 ($\text{EC} \leq 1000$) considered as High-moderate GW recharge, and type-II ($\text{EC} > 1000$) were considered as low GW recharge zones.

Based on the outcomes of the Analytic Hierarchy Process (AHP) model-II, which exhibited a higher accuracy of prediction at 89%, this model was employed for cross-validation. The well locations studied were divided into three categories based on their GW (GW) recharge zones: high,

moderate, and low. Of the 141 wells surveyed, 119 wells (84%) were located in high GW recharge zones, while 17 wells were in moderate zones and 5 wells were in low recharge zones (graphically presented in Figure 7). It indicates that 98 of the 119 wells (82%) located in high GW recharge zones are in agreement, as well as 13 of the 17 wells (76%) in moderate zones, which fall into type-1 wells. Among the 5 wells classified as type-II, 3 (60% agreement) are included in this category. Overall, our study demonstrates a high level of agreement (81%) between electrical conductivity and GW recharge.

5. Conclusion

The study showcases the use of geospatial technology to identify GW recharge potentials in the Quetta region of Pakistan, which is a semi-arid area. The study employed AHP, Fuzzy-AHP, and FR models to assign weights to influencing factors and then reclassified selected thematic maps into three classes based on GW recharge zones. Each class was assigned weights based on its significance to GW recharge, and all layers were combined using an AHP-Weighted linear combination, AHP-Weighted sum, fuzzy-AHP overlay, and FR-based models through ArcGIS. The final map resulted in

three distinct GW recharge potential zones viz; high, moderate, and low GW recharge zone. The following conclusions were derived:

- The maps derived from the various models indicate that the central region constitutes the high GW recharge area, while the southern part is characterized by moderate recharge potential. On the other hand, the zones with low recharge potential are located in the mountains, ridges, and residual hills with steeper slopes and higher elevation, where the infiltration capacity is reduced due to high runoff, leading to a decrease in recharge potential.
- The AHP model-I (weighted overlay), AHP model-II (weighted sum), FAHP model, and FR model demarcated 15%, 39%, 43%, and 42% respectively of an area as high GW recharge
- The validation of GW recharges potential zones maps, created with GIS-based models (AHP, FAHP, and FR), and was conducted using ROC curves. The accuracy of the predictions made by the AHP model-I, AHP model-II, FAHP, and FR models were 84%, 89%, 88%, and 81% respectively. These results indicate that the AHP model-II was the most effective model in this study, outperforming both the FAHP and FR models.

These documents will provide a firsthand and valuable guidance to decision-makers in GW resources management and future planning in land use for urban extension especially in water scarce region. This will also help in implementation of future dug/tube wells or boreholes installation in study area which can minimize the cost and effort of hydrogeological investigation. The study area is situated in a remote and mountainous region, which poses a challenge for the availability of well data. The scarcity of well data, in turn, presents a significant obstacle to the development of robust GW modeling and validation.

References

- [1] Selvam, S., Manimaran, G., Sivasubramanian, P. and Seshunarayana, T., (2014). Geoenvironmental Resource Assessment Using Remote Sensing and GIS: A Case Study from Southern Coastal Region. *Research Journal of Recent Sciences*. Vol. 3(1), 108-115.
- [2] Chandra, S., (2006). *Contribution of Geophysical Properties in Estimating Hydrogeological Parameters of an Aquifer*. Unpublished PhD. Thesis. BHU, Varanasi. 1-197. <http://dx.doi.org/10.13140/2.1.1485.5040>.
- [3] Miller, G. T. and Spoolman, S. E., (2007). *Living in the Environment: Principles, Connections, and Solutions*, 16^{ed}. Thomson Brooks/Cole.
- [4] Gebrie, T., Gadissa, E., Ahmad, I., Dar M. A., Tekla, A. H., Tolosa, A. T., Brhane, E. S. and Fenta, A., (2018). Groundwater Resources Evaluation Using Geospatial Technology. *Environmental Geosciences*, Vol. 25(1), 25-35. <https://doi.org/10.1306/eg.01241817010>.
- [5] Todd, D. K. and Mays, L. W., (2004). *Groundwater Hydrology*. John Wiley and Sons.
- [6] Thakur, D., Bartarya, S. K. and Nainwal, H. C., (2018). Mapping Groundwater Prospect Zones in an Intermontane Basin of the Outer Himalaya in India Using GIS and Remote Sensing Techniques. *Environmental Earth Sciences*, Vol. 77, 1-15. <https://doi.org/10.1007/s12665-018-7552-x>.
- [7] Qureshi, A. S., (2020). Groundwater Governance in Pakistan: From Colossal Development to Neglected Management. *Water*, Vol. 12. <https://doi.org/10.3390/w12113017>.
- [8] Mondal, P. and Dalai, A. K., (2017). *Sustainable Utilization of Natural Resources (Eds.)*. CRC Press.
- [9] Watto, A. (2015). *The Economics of Groundwater Irrigation in the Indus Basin, Pakistan: Tube-well Adoption, Technical and Irrigation Water Efficiency and Optimal Allocation*, Doctoral Dissertation Crawley WA 6009, Australia: University of Western Australia.
- [10] Khan, A. S., Khan, S. D. and Kakar, D. M., (2013). Land Subsidence and Declining Water Resources in Quetta Valley, Pakistan. *Environmental Earth Sciences*, Vol. 70, 2719-2727. <https://doi.org/10.1007/s12665-013-2328-9>.
- [11] Ashraf, M., Routray, J. K. and Saeed, M., (2014). Determinants of Farmers' Choice of Coping and Adaptation Measures to the Drought Hazard in Northwest Balochistan, Pakistan. *Natural Hazards*, Vol. 73, 1451-1473. <https://doi.org/10.1007/s11069-014-1149-9>.
- [12] Ashraf, M. and Routray, J. K., (2015). Spatio-Temporal Characteristics of Precipitation and Drought in Balochistan Province, Pakistan.

- Natural Hazards*, Vol. 77, 229-254. <https://doi.org/10.1007/s11069-015-1593-1>.
- [13] Ali, I. and Aftab, S. M., (2022). Climate Change and Human-Induced Factor Impacts on Quetta Valley Aquifer, Baluchistan, Pakistan. *Journal of Himalayan Earth Sciences*, Vol. 55, 21-45. [http://nceg.uop.edu.pk/GeologicalBulletin/Vol-55\(2\)-2022/Vol-55\(2\)-2022-Paper2.pdf](http://nceg.uop.edu.pk/GeologicalBulletin/Vol-55(2)-2022/Vol-55(2)-2022-Paper2.pdf).
- [14] Ma, Y., (2004). GIS Application in Watershed Management. *Nature and Science*, Vol. 2(2), 1-7. <https://www.sciencepub.net/nature/0202/01ma.pdf>.
- [15] Chen, W., Li, H., Hou, E., Wang, S., Wang, G., Panahi, M., Li, T., Peng, T., Guo, C., Niu, C., Xiao, L., Wang, J. and Ahmad, B. B., (2018). GIS-based Groundwater Potential Analysis Using Novel Ensemble Weights-Of-Evidence with Logistic Regression and Functional Tree Models. *Science of the Total Environment*, Vol. 634, 853-867. <https://doi.org/10.1016/j.scitotenv.2018.04.055>.
- [16] Israil, M., Al-Hadithi, M. and Singhal, D. C., (2006). Application of a Resistivity Survey and geographical Information System (GIS) Analysis for Hydrogeological Zoning of a Piedmont Area. Himalayan Foothill Region, India. *Hydrogeology Journal*, Vol. 14, 753-759. <https://doi.org/10.1007/s10040-005-0483-0>.
- [17] Faust, N., Anderson, W. and Star, J., (1991). Geographic Information Systems and Remote Sensing Future Computing Environment. *Photogrammetric Engineering and Remote Sensing*, Vol. 57, 655-668. https://www.asprs.org/wp-content/uploads/pers/1991journal/jun/1991_jun_655-668.pdf.
- [18] Senthilkumar, M., Gnanasundar, D. and Arumugam, R., (2019). Identifying Groundwater Recharge Zones Using Remote Sensing and GIS Techniques in Amaravathi Aquifer System, Tamil Nadu, South India. *Sustainable Environment Research*, Vol. 29, 1-9. <https://doi.org/10.1186/s42834-019-0014-7>.
- [19] Uc Castillo, J. L., Martínez Cruz, D. A., Ramos Leal, J. A., Tuxpan Vargas, J., Rodríguez Tapia, S. A. and Marín Celestino, A. E., (2022). Delineation of Groundwater Potential Zones (GWPZs) in a Semi-Arid Basin through Remote Sensing, GIS, and AHP Approaches. *Water*, Vol. 14(13). <https://doi.org/10.3390/w14132138>.
- [20] Sardar, H., Akhter, G., Ge, Y. and Haider, S. A., (2022). Delineation of Potential Managed Aquifer Recharge Sites of Kuchlak Sub-Basin, Balochistan, using Remote Sensing and GIS. *Frontiers in Environmental Science*, Vol. 10. <https://doi.org/10.3389/fenvs.2022.916504>.
- [21] Al-Sababhah, N. (2023). The Application of the Analytic Hierarchy Process and GIS to Map Suitable Rainwater Harvesting Sites in (Semi-) Arid Regions in Jordan. *International Journal of Geoinformatics*, Vol. 19(3), 31–44. <https://doi.org/10.52939/ijg.v19i3.2601>.
- [22] Kabeto, J., Adeba, D., Regasa, M. S. and Leta, M. K., (2022). Groundwater Potential Assessment Using GIS and Remote Sensing Techniques: Case Study of West Arsi Zone, Ethiopia. *Water*, Vol. 14(12). <https://doi.org/10.3390/w14121838>.
- [23] Alam, F., Azmat, M., Zarin, R., Ahmad, S., Raziq, A., Young, H. W. V., Nguyen, K. A. and Liou, Y. A., (2022). Identification of Potential Natural Aquifer Recharge Sites in Islamabad, Pakistan, by Integrating GIS and RS Techniques. *Remote Sensing*, Vol. 14(23). <https://doi.org/10.3390/rs14236051>.
- [24] Truong, P., Le, N., Hoang, T., Nguyen, T., Nguyen, T., Kieu, T., Nguyen, T., Izuru, S., Le, V., Raghavan, V., Nguyen, V., and Tran, T. (2023). Climate Change Vulnerability Assessment Using GIS and Fuzzy AHP on an Indicator-Based Approach. *International Journal of Geoinformatics*, Vol. 19(2), 39–53. <https://doi.org/10.52939/ijg.v19i2.2565>.
- [25] Hayat, S., Szabó, Z. and Tóth, Á., (2021). MAR Site Suitability Mapping for Arid–Semiarid Regions by Remote Data and Combined. *Acque Sotterranee - Italian Journal of Groundwater*, Vol. 10, 17-28. <https://doi.org/10.7343/as-2021-505>.
- [26] Mohd Rasu, M., Suhandri, H., Khalifa, N., Abdul Rasam, A., and Hamid, A. (2023). Evaluation of Flood Risk Map Development through GIS-Based Multi-Criteria Decision Analysis in Maran District, Pahang - Malaysia. *International Journal of Geoinformatics*, Vol. 19(10), 1–16. <https://doi.org/10.52939/ijg.v19i9.2873>.
- [27] Tazi, M., El Azzab, D., El Moutaouakkil, N., and Charroud, M. (2024). Integration of Geospatial Technologies and Fuzzy-AHP Analysis to Assess Groundwater Potential in the Sirwa Massif, Anti-Atlas Region, Morocco. *International Journal of Geoinformatics*, Vol. 20(5), 79–94. <https://doi.org/10.52939/ijg.v20i5.3235>.
- [28] Argaz, A., Ouahman, B., Darkaoui, A., Bikhtar, H., Yabsa, K. and Laghzal, A., (2019). Application of Remote Sensing

- Techniques and GIS-Multicriteria Decision Analysis for Groundwater Potential Mapping in Souss Watershed, Morocco. *Environmental Sciences*, Vol. 10, 411-421. https://www.jmaterenvirosnci.com/Document/vol10/vol10_N5/42-JMES-Argaz-2019.pdf.
- [29] Patil, S. G. and Mohite, N. M., (2014). Identification of Groundwater Recharge Potential Zones for a Watershed Using Remote Sensing and GIS. *International Journal of Geomatics and Geosciences*, Vol. 4, 485-498.
- [30] Dabral, S., Bhatt, B., Joshi, J. P. and Sharma, N., (2014). Groundwater suitability Recharge Zones Modelling – A GIS Application. *The International Archives of the Photogrammetry, Remote Sensing and Spatial Information Sciences*, Vol. XL-8, 347-353. <https://doi.org/10.5194/isprsarchives-XL-8-347-2014>.
- [31] Razandi, Y., Pourghasemi, H. R., Neisani, N. S. and Rahmati, O., (2015). Application of Analytical Hierarchy Process, Frequency Ratio, and Certainty Factor Models for Groundwater Potential Mapping Using GIS. *Earth Science Informatics*, Vol. 8, 867-883. <https://doi.org/10.1007/s12145-015-0220-8>.
- [32] Ahmed, A. A. and Shabana, A. R., (2020). Integrating of Remote Sensing, GIS and Geophysical Data for Recharge Potentiality Evaluation in Wadi El Tarfa, Eastern Desert, Egypt. *Journal of African Earth Sciences*, Vol. 172. <https://doi.org/10.1016/j.jafrearsci.2020.103957>.
- [33] Ahmed, R. and Sajjad, H., (2018). Analyzing Factors of Groundwater Potential and its Relation with Population in the Lower Barpani Watershed, Assam, India. *Natural Resources Research*, Vol. 27, 503-515. <https://doi.org/10.1007/s11053-017-9367-y>.
- [34] Freeze, R. A., (1984). *Groundwater Contamination*. ed: Wiley Online Library.
- [35] Jerbi, H., Massuel, S., Leduc, C. and Tarhouni, J., (2018). Assessing Groundwater Storage in the Kairouan Plain Aquifer Using a 3D Lithology Model (Central Tunisia). *Arabian Journal of Geosciences*, Vol. 11, 1-10. <https://doi.org/10.1007/s12517-018-3570-y>.
- [36] Tolche, A. D., (2021). Groundwater Potential Mapping Using Geospatial Techniques: A Case Study of Dhungeta-Ramis Sub-Basin, Ethiopia. *Geology, Ecology, and Landscapes*, Vol. 5, 65-80. <https://doi.org/10.1080/24749508.2020.1728882>.
- [37] El-Sawy, K., Ibrahim, A. M., El-Bastawesy, M. A. and El-Saud, W. A., (2016). Automated, Manual Lineaments Extraction and Geospatial Analysis for Cairo-Suez District (Northeastern Cairo-Egypt), Using Remote Sensing and GIS. *International Journal of Innovative Science, Engineering and Technology*, Vol. 3, 491-500. <https://www.researchgate.net/publication/349338660>.
- [38] Das, S., (2019). Comparison among Influencing Factor, Frequency Ratio, and Analytical Hierarchy Process Techniques for Groundwater Potential Zonation in Vaitarna basin, Maharashtra, India. *Groundwater for Sustainable Development*, Vol. 8, 617-629. <https://doi.org/10.1016/j.gsd.2019.03.003>.
- [39] Maidment, D. R., (1993). *Handbook of hydrology*: McGraw-Hill.
- [40] Simmers, I., (1990). *Aridity, Groundwater Recharge and Water Resources Management, Groundwater Recharge. A Guide to Understanding the Natural Recharge*. Hannover: Ed. R. van Acken GmbH, 1-20.
- [41] Chaplot, V. and Le Bissonnais, Y., (2000). Field Measurements of Interrill Erosion Under Different Slopes and Plot Sizes. *Earth Surface Processes and Landforms: The Journal of the British Geomorphological Research Group*, Vol. 25, 145-153.
- [42] Essig, E. T., Corradini, C., Morbidelli, R. and Govindaraju, R. S., (2009). Infiltration and Deep Flow Over Sloping Surfaces: Comparison of Numerical and Experimental Results. *Journal of Hydrology*, Vol. 374, 30-42. <https://doi.org/10.1016/j.jhydrol.2009.05.017>.
- [43] Yuan, J. P., Lei, T. W., Guo, S. Y. and Jiang, D. S., (2001). Study on Spatial Variation of Infiltration Rates for Small Watershed in Loess Plateau. *J Hydraul Eng*, Vol. 10, 88-92.
- [44] Liu, J., Gao, G., Wang, S., Jiao, L., Wu, X. and Fu, B., (2018). The Effects of Vegetation on Runoff and Soil Loss: Multidimensional Structure Analysis and Scale Characteristics. *Journal of Geographical Sciences*, Vol. 28, 59-78. <https://doi.org/10.1007/s11442-018-1459-z>.
- [45] Szymura, T. H. and Szymura, M., (2017). Topographic Wetness Index Explains Soil Moisture Better than Bioindication with Ellenberg's Indicator Values. *Ecological Indicators*, Vol. 85, 172-179. <https://doi.org/10.1016/j.ecolind.2017.10.011>.
- [46] Nampak, H., Pradhan, B. and Abd Manap, M., (2014). Application of GIS Based Data Driven Evidential Belief Function Model to Predict Groundwater Potential Zonation. *Journal of*

- Hydrology*, Vol. 513, 283-300. <https://doi.org/10.1016/j.jhydrol.2014.02.053>.
- [47] Yıldırım, Ü., (2021). Identification of Groundwater Potential Zones Using GIS and Multi-Criteria Decision-Making Techniques: A Case Study Upper Coruh River Basin (NE Turkey). *ISPRS International Journal of Geo-Information*, Vol. 10. <https://doi.org/10.3390/ijgi10060396>.
- [48] Arulbalaji, P., Padmalal, D. and Sreelash, K., (2019). GIS and AHP Techniques Based Delineation of Groundwater Potential Zones: A Case Study from Southern Western Ghats, India. *Scientific Reports*, Vol. 9. <https://doi.org/10.1038/s41598-019-38567-x>.
- [49] Carlston, C. W., (1963). *Drainage Density and Streamflow*. Geological Survey Professional Paper 422-C.
- [50] Selvam, S., Dar, F. A., Magesh, N. S., Singaraja, C., Venkatramanan, S. and Chung, S. Y., (2016). Application of Remote Sensing and GIS for Delineating Groundwater Recharge Potential Zones of Kovilpatti Municipality, Tamil Nadu using IF technique. *Earth Science Informatics*, Vol. 9, 137-150. <https://doi.org/10.1007/s12145-015-0242-2>.
- [51] Adiat, K. A. N., Nawawi, M. N. M. and Abdullah, K., (2012). Assessing the Accuracy of GIS-based Elementary Multi Criteria Decision Analysis as a Spatial Prediction Tool—A Case of Predicting Potential Zones of Sustainable Groundwater Resources. *Journal of Hydrology*, Vol. 440, 75-89. <https://doi.org/10.1016/j.jhydrol.2012.03.028>.
- [52] Arshad, A., Zhang, Z., Zhang, W. and Dilawar, A., (2020). Mapping Favorable Groundwater Potential Recharge Zones using a GIS-based Analytical Hierarchical Process and Probability Frequency Ratio Model: A Case Study from an Agro-Urban Region of Pakistan. *Geoscience Frontiers*, Vol. 11(5), 1805-1819. <https://doi.org/10.1016/j.gsf.2019.12.013>.
- [53] Harinarayana, P., Gopalakrishna, G. S. and Balasubramanian, A., (2000). Remote Sensing Data for Groundwater Development and Management in Keralapura Watersheds of Cauvery Basin, Karnataka, India. *Indian Mineral*, Vol. 34, 11-17. https://www.researchgate.net/publication/308673710_Remote_sensing_data_for_groundwater_development_and_management_in_Keralapura_Watersheds_of_Cauvery_basin_Karnataka_India.
- [54] Saranya, T. and Saravanan, S., (2020). Groundwater Potential Zone Mapping Using Analytical Hierarchy Process (AHP) and GIS for Kancheepuram District, Tamilnadu, India. *Modeling Earth Systems and Environment*, Vol. 6, 1105-1122. <https://doi.org/10.1007/s40808-020-00744-7>.
- [55] Khan, A., Govil, H., Taloor, A. K. and Kumar, G., (2020). Identification of Artificial Groundwater Recharge Sites in Parts of Yamuna River Basin India Based on Remote Sensing and Geographical Information System. *Groundwater for Sustainable Development*, Vol. 11. <https://doi.org/10.1016/j.gsd.2020.100415>.
- [56] Chowdhury, A., Jha, M. K. and Chowdary, V. M., (2010). Delineation of Groundwater Recharge Zones and Identification of Artificial Recharge Sites in West Medinipur District, West Bengal, Using RS, GIS and MCDM Techniques. *Environmental Earth Sciences*, Vol. 59, 1209-1222. <https://doi.org/10.1007/s12665-009-0110-9>.
- [57] Magesh, N. S., Chandrasekar, N. and Soundranayagam, J. P., (2012). Delineation of Groundwater Potential Zones in Theni District, Tamil Nadu, Using Remote Sensing, GIS and MIF Techniques. *Geoscience Frontiers*, Vol. 3, 189-196. <https://doi.org/10.1016/j.gsf.2011.10.007>.
- [58] Srivastava, P. K. and Bhattacharya, A. K., (2006). Groundwater Assessment through an Integrated Approach Using Remote Sensing, GIS and Resistivity Techniques: A Case Study from a Hard Rock Terrain. *International Journal of Remote Sensing*, Vol. 27, 4599-4620. <https://doi.org/10.1080/01431160600554983>.
- [59] Yeh, H. F., Lee, C. H., Hsu, K. C. and Chang, P. H., (2009). GIS for the Assessment of the Groundwater Recharge Potential Zone. *Environmental Geology*, Vol. 58, 185-195. <https://doi.org/10.1007/s00254-008-1504-9>.
- [60] Gebreyohannes, T., De Smedt, F., Walraevens, K., Gebresilassie, S., Hussien, A., Hagos, M., Amare, K., Deckers, J. and Gebrehiwot, K., (2017). Regional Groundwater Flow Modeling of the Geba Basin, Northern Ethiopia. *Hydrogeology Journal*, Vol. 25, 639-65. <https://doi.org/10.1007/s10040-016-1522-8>.
- [61] Singh, A., Panda, S. N., Kumar, K. S. and Sharma, C. S., (2013). Artificial Groundwater Recharge Zones Mapping Using Remote Sensing and GIS: A Case Study in Indian Punjab. *Environmental Management*, Vol. 52,

- 61-71. <https://doi.org/10.1007/s00267-013-0101-1>.
- [62] Kotchoni, D. V., Vouillamoz, J. M., Lawson, F. M., Adjomayi, P., Boukari, M. and Taylor, R. G., (2018). Relationships between Rainfall and Groundwater Recharge in Seasonally Humid Benin: A Comparative Analysis of Long-Term Hydrographs in Sedimentary and Crystalline Aquifers. *Hydrogeology Journal*, Vol. 27, 447–457. <https://doi.org/10.1007/s10040-018-1806-2>.
- [63] Mahalingam, B. and Vinay, M., (2015). Identification of Ground Water Potential Zones Using GIS and Remote Sensing Techniques: A Case Study of Mysore Taluk-Karnataka. *International Journal of Geomatics and Geosciences*, Vol. 5, 393-403. https://www.academia.edu/10224832/Identification_of_ground_water_potential_zones_using_GIS_and_Remote_Sensing_Techniques_A_case_study_of_Mysore_taluk_Karnataka.
- [64] Saaty, T. L., (1980). *The Analytical Hierarchy Process, Planning, Priority, Resource Allocation*. RWS Publications, USA.
- [65] Arshad, A., Zhang, Z., Zhang, W. and Dilawar, A., (2020). Mapping Favorable Groundwater Potential Recharge Zones Using a GIS-Based Analytical Hierarchical Process and Probability Frequency Ratio Model: A Case Study from an Agro-Urban Region of Pakistan. *Geoscience Frontiers*, Vol. 11, 1805-1819. <https://doi.org/10.1016/j.gsf.2019.12.013>.
- [66] Malczewski, J., (1999). *GIS and Multicriteria Decision Analysis*. John Wiley & Sons.
- [67] Brunelli, M., (2014). *Introduction to the Analytic Hierarchy Process*. Springer: Amsterdam, The Netherlands, 2015. <http://dx.doi.org/10.1007/978-3-319-12502-2>.
- [68] Zadeh, L. A., (1965). Fuzzy Sets. *Information and Control*, Vol. 8, 338-353.
- [69] Tiwari, A. K., Lavy, M., Amanzio, G., De Maio, M., Singh, P. K. and Mahato, M. K., (2017). Identification of Artificial Groundwater Recharging Zone using a GIS-based Fuzzy Logic Approach: A Case Study in a Coal Mine Area of the Damodar Valley, India. *Applied Water Science*, Vol. 7, 4513-4524. <https://doi.org/10.1007/s13201-017-0603-8>.
- [70] Mallick, J., Khan, R. A., Ahmed, M., Alqadhi, S. D., Alsubih, M., Falqi, I. and Hasan, M. A., (2019). Modeling Groundwater Potential Zone in a Semi-Arid Region of Aseer Using Fuzzy-AHP and Geoinformation Techniques. *Water*, Vol. 11. <https://doi.org/10.3390/w11122656>.
- [71] Buckley, J. J., (1985). Fuzzy Hierarchical Analysis. *Fuzzy Sets and Systems*, Vol. 17, 233-247.
- [72] Githinji, T. W., Dindi, E. W., Kuria, Z. N. and Olago, D. O., (2022). Application of Analytical Hierarchy Process and Integrated Fuzzy-Analytical Hierarchy Process for Mapping Potential Groundwater Recharge Zone Using GIS in the Arid Areas of Ewaso Ng'iro–Lagh Dera Basin, Kenya. *HydroResearch*, Vol. 5, 22-34. <https://doi.org/10.1016/j.hydres.2021.11.001>.
- [73] Aouragh, M. H., Essahlaoui, A., El Ouali, A., El Hmaidi, A. and Kamel, S., (2017). Groundwater Potential of Middle Atlas Plateaus, Morocco, Using Fuzzy Logic Approach, GIS and Remote Sensing. *Geomatics, Natural Hazards and Risk*, Vol. 8, 194-206. <https://doi.org/10.1080/19475705.2016.1181676>.
- [74] Oh, H. J., Kim, Y. S., Choi, J. K., Park, E. and Lee, S., (2011). GIS Mapping of Regional Probabilistic Groundwater Potential in the Area of Pohang City, Korea. *Journal of Hydrology*, Vol. 399, 158-172. <https://doi.org/10.1016/j.jhydrol.2010.12.027>.
- [75] Ozdemir, A., (2011). GIS-based Groundwater Spring Potential Mapping in the Sultan Mountains (Konya, Turkey) Using Frequency Ratio, Weights of Evidence and Logistic Regression Methods and their Comparison. *Journal of Hydrology*, Vol. 411, 290-308. <https://doi.org/10.1016/j.jhydrol.2011.10.010>.
- [76] Manap, M. A., Nampak, H., Pradhan, B., Lee, S., Sulaiman, W. N. A. and Ramli, M. F., (2014). Application of Probabilistic-Based Frequency Ratio Model in Groundwater Potential Mapping Using Remote Sensing Data and GIS. *Arabian Journal of Geosciences*, Vol. 7, 711-724. <https://doi.org/10.1007/s12517012-0795-z>.
- [77] Moghaddam, D. D., Rezaei, M., Pourghasemi, H. R., Pourtaghie, Z. S. and Pradhan, B., (2015). Groundwater Spring Potential Mapping Using Bivariate Statistical Model and GIS in the Taleghan watershed, Iran. *Arabian Journal of Geosciences*, Vol. 8, 913-929. <https://doi.org/10.1007/s12517-013-1161-5>.
- [78] Pourtaghi, Z. S. and Pourghasemi, H. R., (2014). Avaliação e mapeamento do potencial em nascentes de água subterrânea com base em SIG no município de Birjand, sul da Província de Khorasan, Irão. *Hydrogeology Journal*, Vol. 22, 643-662. <https://doi.org/10.1007/s10040-013-1089-6>.

- [79] Ahmed, A., Ranasinghe-Arachchilage, C., Alrajhi, A. and Hewa, G., (2021). Comparison of Multicriteria Decision-Making Techniques for Groundwater Recharge Potential Zonation: Case Study of the Willochra Basin, South Australia. *Water*, Vol. 13. <https://doi.org/10.3390/w13040525>.
- [80] Brady, N. C., Weil, R. R. and Weil, R. R., (2008). *The Nature and Properties of Soils*. Upper Saddle River, NJ: Prentice Hall. Vol. 13, 662-710.
- [81] FitzPatrick, E. A., (1978). An Introduction to Soil Science. *Soil Science*, Vol. 125. https://journals.lww.com/soilsci/citation/1978/04000/an_introduction_to_soil_science.18.aspx
- [82] De Wit, P. V. and Nachtergaele, F. O., (1990). *Explanatory Note on the Soil Map of the Republic of Botswana*. Annex 1: Typifying pedons and soil analytical data.
- [83] Driessen, P. M. and Dudal, R., (1989). *Lecture Notes on the Geography, Formation, Properties and Use of the Major Soils of the World* (Eds). Agricultural Univ., Department of Soil Science & Geology.
- [84] Kaliraj, S., Chandrasekar, N. and Magesh, N. S., (2015). Evaluation of Multiple Environmental Factors for Site-Specific Groundwater Recharge Structures in the Vaigai River Upper Basin, Tamil Nadu, India, Using GIS-based Weighted Overlay Analysis. *Environmental Earth Sciences*, Vol. 74, 4355-4380. <https://doi.org/10.1007/s12665-015-4384-9>.
- [85] Shaban, A., Khawlie, M. and Abdallah, C., (2006). Use of Remote Sensing and GIS to Determine Recharge Potential Zones: The Case of Occidental Lebanon. *Hydrogeology Journal*, Vol. 14, 433-443. <https://doi.org/10.1007/s10040-005-0437-6>.
- [86] Shaban, A., Khawlie, M. and Abdallah, C., (2006). Remote Sensing and GIS for Artificial Recharge Study, Runoff Estimation and Planning in Ayyar Basin, Tamil Nadu, India. *Environmental Geology*, Vol. 48, 158-170. <https://doi.org/10.1007/s00254-005-1284-4>.
- [87] Boughariou, E., Allouche, N., Ben Brahim, F., Nasri, G. and Bouri, S., (2021). Delineation of groundwater Potentials of Sfax Region, Tunisia, Using Fuzzy Analytical Hierarchy Process, Frequency Ratio, and Weights of Evidence Models. *Environment, Development and Sustainability*, Vol. 23, 14749-14774. <https://doi.org/10.1007/s10668-021-01270-x>.
- [88] Elvis, B. W. W., Arsene, M., Theophile, N. M., Bruno, K. M. E. and Olivier, O. A., (2022). Integration of Shannon Entropy (SE), Frequency Ratio (FR) and Analytical Hierarchy Process (AHP) in GIS for Suitable Groundwater Potential Zones Targeting in the Yoyo River Basin, Méiganga Area, Adamawa Cameroon. *Journal of Hydrology: Regional Studies*, Vol. 39. <https://doi.org/10.1016/j.ejrh.2022.100997>.
- [89] Yesilnacar, E. and Topal, T. A. M. E. R., (2005). Landslide Susceptibility Mapping: A Comparison of Logistic Regression and Neural Networks Methods in a Medium Scale Study, Hendek Region (Turkey). *Engineering Geology*, Vol. 79, 251-266. <https://doi.org/10.1016/j.enggeo.2005.02.002>.
- [90] Pourtaghi, Z. S. and Pourghasemi, H. R., (2014). GIS-Based Groundwater Spring Potential Assessment and Mapping in the Birjand Township, Southern Khorasan Province, Iran. *Hydrogeol J*, Vol. 22(3), 643-662. <https://doi.org/10.1007/s10040-013-1089-6>.
- [91] Njumbe, L. J. N., Lordon, A. E. D. and Agyingi, C. M., (2023). Determination of Groundwater Potential Zones on the Eastern Slope of Mount Cameroon Using Geospatial Techniques and Seismoelectric Method. *SN Applied Sciences*, Vol. 5(9). <https://doi.org/10.1007/s42452-023-05458-w>.
- [92] Hem, J. D., (1985). *Study and Interpretation of the Chemical Characteristics of Natural Water*, Department of the Interior, US Geological Survey.
- [93] Sarath Prasanth, S. V., Magesh, N. S., Jitheshlal, K. V., Chandrasekar, N. and Gangadhar, K. J. A. W. S. (2012). Evaluation of Groundwater Quality and its Suitability for Drinking and Agricultural Use in the Coastal Stretch of Alappuzha District, Kerala, India. *Applied Water Science*, Vol. 2, 165-175. <https://doi.org/10.1007/s13201-012-0042-5>.